2022-12-01

Identifying Particulate Matter Spatial Variation In The El Paso Del Norte Region Using Land-Use Regression Modeling And Data Obtained From A Network Of Low-Cost Sensors

Leonardo Demetrio Vazquez-Raygoza
University of Texas at El Paso

IDENTIFYING PARTICULATE MATTER SPATIAL VARIATION IN THE EL PASO DEL NORTE REGION USING LAND-USE REGRESSION MODELING AND DATA OBTAINED FROM A NETWORK OF LOW-COST SENSORS

Leonardo Demetrio Vazquez-Raygoza

Master's Program in Civil Engineering

APPROVED:

Wen-Whai Li, Ph.D., PE, Chair

Mayra Chavez, Ph.D., EIT

Soyoung Jeon, Ph.D.

Stephen L. Crites, Jr., Ph.D.
Dean of the Graduate School

DEDICATION

To Monica and Hector, thank you for all your love and patience, and to Mar, thank you for your kindness, love, and compassion, I could not have done this without you.

IDENTIFYING PARTICULATE MATTER SPATIAL VARIATION IN THE EL PASO DEL NORTE REGION USING LAND-USE REGRESSION MODELING AND DATA OBTAINED FROM A NETWORK OF LOW-COST SENSORS

by

Leonardo Demetrio Vazquez-Raygoza, BS

THESIS

Presented to the Faculty of the Graduate School of

The University of Texas at El Paso

in Partial Fulfillment

of the Requirements

for the Degree of

MASTER OF SCIENCE

Department of Civil Engineering

THE UNIVERSITY OF TEXAS AT EL PASO

December 2022

ACKNOWLEDGMENTS

I want to extend my deepest gratitude to my advisor and mentor, Dr. Wen-Whai Li, for allowing me to join his research team; his guidance, patience, and expertise have helped me further my academic career and have better prepared me for a future in research. Furthermore, I wish to extend my sincerest gratitude to Dr. Mayra Chavez for her support and guidance; her feedback and advice have been essential in developing this thesis and growing as an induvial. I would also like to thank Dr. Soyoung Jeon, whose expertise and guidance was essential in developing the land use regression model; thank you for your guidance and time.

I would also like to thank my family, whose kindness and encouragement have guided me through this journey. To my mother and father, thank you for your unwavering faith in me; your guidance and advice have helped me grow as an individual. My aunt Miriam for her patience and kind words. To my grandparents, Dina and Mario, for their remarkable, selfless generosity. Most of all, I would like to thank my beautiful fiancée, Mar. You have always been there for me, both good and bad. You have shown me kindness, love, support, and patience, which have been essential in my growth as an individual.

This project was partially supported by a grant from the Texas Commission on Environmental Quality and the U.S. Department of Transportation through the Center for Advancing Research in Transportation Emissions, Energy, and Health (CARTEEH). I want to thank the El Paso Independent School District staff for assisting in setting up and deploying the sensors on their campuses. I would also like to thank the Universidad Autonoma de Ciudad Juarez for their efforts in this project. The contents of this thesis are solely the responsibility of the authors and do not represent the official views of the Texas Commission on Environmental Quality and the U.S. Department of Transportation.

ABSTRACT

The emergence and rise in popularity of low-cost sensors for atmospheric observation are setting a new precedent in identifying emission hotspots and providing high-resolution spatial and temporal data. Furthermore, low-cost sensors are becoming popular among institutions and the public, allowing community scientists to become more involved in air quality monitoring. However, concerns about the accuracy and precision of low-cost sensors have been questioned. Most recent research has focused on the utility of real-time monitoring and calibration requirements for these sensors. A low-cost monitoring project has deployed sensors in the El Paso del Norte region in low and high annual average daily traffic (AADT), school, and industrial zones. A calibration equation was created for each sensor during a two-week deployment next to a federal monitoring station; the low-cost sensors showed a high coefficient of determination (R2) of >0.9 for PM2.5 between low-cost sensors and monitoring stations. During the two months that the sensors were in the field, PM2.5 values had a higher concentration in the high AADT zone and higher concentrations in the low AADT zones in Cd. Juarez. The PM values recorded at each site were utilized in the land use regression model to find variables that significantly affected PM concentration. While traffic variables showed an adverse effect on PM, PM concentration would increase per mile decrease to a traffic source; geographic data showed an increase in PM per unit increase in population at a given 500 m buffer zone.

TABLE OF CONTENTS

ACKNOWLEDGMENTS v

ABSTRACT vi

LIST OF TABLES ix

LIST OF FIGURES x

CHAPTER 1: INTRODUCTION 1

1.1. INTRODUCTION 1

1.2. PROBLEM STATEMENT 2

1.3. OBJECTIVES 3

1.4. SIGNIFICANCE OF THE WORK 4

CHAPTER 2: LITERATURE REVIEW 5

2.1 AIR POLLUTION IN EL PASO DEL NORTE REGION 5

2.1.1 PARTICULATE MATTER 8

2.2 NEAR-ROAD COMMUNITY EXPOSURES 12

2.3 LOW-COST SENSORS 13

2.3.1 LOW-COST SENSOR OPERATING CONCERNS 15

2.3.2 LOW-COST SENSOR PERFORMANCE 16

2.3.3 LOW-COST SENSOR CALIBRATION TECHNIQUES 25

CHAPTER 3 STUDY DESIGN 30

3.1. SCIENTIFIC APPROACH 30

3.2. SELECTION OF THE SITE LOCATION 31

3.2.1 LOW-COST NETWORK EXPERIMENTAL DESIGN IN EL PASO DEL NORTE 31

3.3. SELECTION OF LOW-COST SENSORS 35

3.4. LOW-COST SENSORS DATA COLLECTION 37

3.5. LOW-COST SENSOR DATA VALIDATION 38

3.6. COLLOCATED SENSORS PRE-DEPLOYMENT 41

3.7. REGRESSION MODELS FOR SENSOR CORRECTION FACTOR 41

3.8. LAND-USE REGRESSION MODELING 42

3.8.1 OPENSTREETMAP 43

CHAPTER 4: STATISTICAL METHODS....44
4.1 LINEAR REGRESSION ANALYSIS....44
4.2 MULTIPLE REGRESSION MODEL....44
CHAPTER 5: LOW-COST SENSOR CALIBRATION AND QUALITY CONTROL....46
5.1. SIDE-BY-SIDE COMPARISON LOW-COST SENSOR AND TCEQ CAMS STATION....46
5.2 INTERCHANNEL COMPARISON FOR LOW-COST SENSORS....48
5.3 SENSOR TO SENSOR COMPARISON....51
CHAPTER 6: LAND USE REGRESSION MODELING....53
6.1. LAND USE REGRESION MODELING CONSIDERATIONS....53
6.2. VARIABLES SELECTED FOR LUR MODELING....54
CHAPTER 7: RESULTS AND DISCUSSIONS....58
7.1. LOW-COST SENSOR PERFORMANCE IN THE EL PASO DEL NORTE REGION....58
7.1.1 $PM_{2.5}$ IN THE EL PASO DEL NORTE REGION....58
7.1.2 DIURNAL $PM_{2.5}$ VARIATION....60
7.1.3 METEOROLOGICAL DATA IN THE EL PASO DEL NORTE REGION....63
7.2. LAND USE REGRESSION MODELING OUTPUT....68
CHAPTER 8: CONCLUSIONS AND RECOMMENDATIONS....74
8.1 LOW-COST SENSOR PERFORMANCE....74
8.2. LAND-USE REGRESSION MODELING....75
8.3. FURTHER RESEARCH....75
REFERENCES....77
APPENDIX....87
VITA....90

LIST OF TABLES

Table 1: NAAQS Table for $PM_{2.5}$ and PM_{10} 11
Table 2: El Paso Area: Attainment Status for $PM_{2.5}$ and PM_{10} 11
Table 3: Research on Low-Cost Sensors 20
Table 4: Multiple Regression PurpleAir Sensors Model Values of Betas 28
Table 5: PurpleAir Name of Site and Sensor 34
Table 6: Purple Air Sensor Evaluation By AQ-SPEC's Laboratories 37
Table 7: Operating Range PurpleAir-II 38
Table 8: Low-Cost Sensor Number of online and invalidated hours during the study period 40
Table 9: Correlation between Low-Vost Sensors and CAMS12 48
Table 10: Inter-Channel R2 for Low-Cost Sensor 50
Table 11: Low-Cost Sensors Duplicated Sensors Inter-Channel R^2 52
Table 12: Land Use Regression Variables Univariate Analysis against $PM_{2.5}$ Variables 55
Table 13: Land Use Regression Variables Univariate Analysis against PM_{10} Variables 56
Table 14: Summary Statistics of $PM_{2.5}$ in El Paso and Cd. Juarez 59
Table 15: $PM_{2.5}$ Daily Highest Concentration throughout the week 62
Table 16.:Temperature Summary Statistics in El Paso and Cd. Juarez 64
Table 17: Summary Statistics Relative Humidity 66
Table 18: Generalized Linear Model for $PM_{2.5}$ using selected LUR Variables 69
Table 19: Generalized Linear Model for PM_{10} with LUR variables 71
Table 20: Generalized Linear Model II for PM2.5 using LUR variables that have a higher affinity with PM2.5 72
Table 21: Generalized Linear Model II for PM_{10} using selected LUR variables 73
Table 22: PM_{10} Summary Statistics 87

LIST OF FIGURES

Figure 1: Pollutant over El Paso and Cd. Juarez 8
Figure 2: Size Distribution of $PM_{2.5}$ and PM_{10} 9
Figure 3: Low-Cost Sensors Location in El Paso del Norte 32
Figure 4: Roads in El Paso del Norte 32
Figure 5: PA-II-SD internal components and external view 35
Figure 6: PA-II-SD deployed next to TCEQ CAMS 12 Station 46
Figure 7: Scatter Plot Matrix of Selected LUR Variables 57
Figure 8: Daily PM2.5 Boxplots 60
Figure 9: Wind Roses in the El Paso Del Norte 67
Figure 10: Diurnal Variation Box Plots For El Paso Texas 88
Figure 11: Diurnal Variation Box Plots for Cd. Juarez Mexico 89

CHAPTER 1: INTRODUCTION

1.1. INTRODUCTION

Particulate matter comes from many sources and poses a significant health risk. For example, wind erosion is a notable environmental factor from natural environments that causes an increase in dust emissions and produces severe particulate air pollution [1], [2]. Wind erosion is significant in highly arid climates such as The El Paso Del Norte Region (PdN), which encompasses the cities of El Paso, Texas, and Cd. Juarez, Chihuahua [3]. These communities also face air quality issues from burgeoning growth and industrialization, which further pressure local governments to protect their residents' respiratory health. This multifaceted rapid decrease in air quality is due to an increase in aeolian processes over the last decades, which are a direct response to environmental dust stresses, global climate change, and other anthropogenic changes [4]. In addition, an increase in urban sprawl has worsened road conditions (paved or unpaved) and caused elevated traffic levels, influencing fine and coarse PM levels [5].

El Paso's complex topography plays a pivotal role in air pollution. For example, El Paso shares an air basin encapsulated by El Paso's Franklin Mountains, Sierra de Juarez, and Dona Ana County. Environmental factors such as the Rio Grande River and the expansive mountain ranges are defining features of the air basin, which greatly influence wind patterns across the sister cities of El Paso and Cd. Juarez. Since the mid-1990, the US and Mexico have cooperated in assessing many of the air quality problems in the region [6]. The PdN has been a large area of interest due to the shared air shed between El Paso and Cd. Juarez. The border cities have primarily been of interest due to their unique environment, increased vehicular crossing, and rapid expansion.

The rapid urbanization of both El Paso and Cd. Juarez has created many environmental issues, and public infrastructure is unable to keep-up, causing an increase in comorbidities for residents. Mass migration and inequality issues have hindered efforts to address these concerns. Thus, although rapid urbanization has created a global manufacturing hub, it has also led to a rapid deterioration in the air quality within the PdN air basin. Current federal monitoring stations are not

enough to capture every change and hotspot within a city, as their range is limited to their fixed location, sparking global interest in equipment lower in cost and readily available.

Low-cost sensors have the potential to dictate when and where air pollution monitoring can be conducted. Recent technological advancements have allowed the emergence of low-cost monitoring sensors (≤ $500), which provide a large spatial and temporal resolution due to their compact size and availability to the public. As a result, low-cost sensors have gained traction over the past few years from the academic and public sectors to involve citizens in air monitoring and access areas that could benefit from having a reference station.

This thesis assesses the viability of a low-cost monitoring network and how it can help supplement data from reference stations. Currently, reference stations have limited spatial and temporal variability. As a result, they may not be able to capture region-specific pollutant events; as such, a low-cost network could help provide a greater degree of variability and be used to access areas that do not have access to reference stations. Furthermore, regulatory monitoring stations are costly to introduce and maintain, whereas a low-cost sensor is quick to deploy, and maintenance cost is minimal. While several environmental issues stem from rapid, unsustainable industrialization, this thesis will solely concentrate on its effects on air pollution monitoring. Air pollution will be assessed through the low-cost sensor network and evaluated with a Texas Commission on Environmental Quality (TCEQ) monitoring station.

1.2. PROBLEM STATEMENT

Atmospheric contamination, especially particulate matter (PM), is a well-established environmental health risk factor[7], [8]. For instance, long- and short-term exposure to PM has been shown to increase the risks of cardiovascular and respiratory diseases, further aggravating comorbidities and causing mortality rates to rise [9]–[12].

Exposure assessment of $PM_{2.5}$ (particles with an aerodynamic diameter of 2.5 μm) has relied mainly on regulatory monitoring stations, which state and local agencies maintain. For

example, the Texas Commission on Environmental Equality (TCEQ) maintains monitoring stations in the El Paso del Norte Region. The operations of these continuous ambient monitoring stations (CAMS) have utilized high-quality air monitoring instruments and followed a standardized data quality assurance procedure that provides $PM_{2.5}$ data of a "gold-standard" quality. However, CAMs stations are sparse within a city primarily due to their high operating costs and strict quality measures. Therefore, the sparsity of these monitoring stations limits a city's ability to accurately reflect PM concentrations due to the high temporal variation of PM. The monitoring scarcity also prevents models and exposure estimates from accurately reflecting air pollution within a given area [13]. Therefore, low-cost sensors can provide a more detailed overview of a city instead of a small section.

This research attempts to fill in the gaps of the CAMs station by creating a network of community monitors that could complement regulatory monitors. Through community monitoring, exposure models can further supplement monitoring stations and encompass a larger spatiotemporal region. In addition, these low-cost sensors could be used with federal monitoring sites, allowing for more cohesive exposure analysis.

1.3. OBJECTIVES

This research attempts to create a land-use regression model (LUR) based on PM patterns observed by a set of low-cost PM sensors in the El Paso del Norte Region. Environmental characteristics influencing PM concentrations are used to find the pollutant's dispersion and intensity over a given area. The land use regression model uses a network of monitors to develop a stochastic model using predictor variables such as roads, green spaces, and population [14].

The tasks of this research include:

1.) Comparing low-cost sensors with Federal Reference Method/ Federal Equivalent Methods (FRM/FEM) monitors at a given CAMs station.

2.) Deploying low-cost sensors at predetermined locations to create a community network.

3.) Gathering Land Use Regression Variables

4.) Correcting and evaluating data for the use of LUR modeling.

1.4. SIGNIFICANCE OF THE WORK

The deployment of low-cost sensors around the community will more accurately track exposure concentrations to PM and improve models that previously only utilized federal monitoring stations. The LUR model will also use a large volume of data gathered from the low-cost sensor and open data sources to give a better exposure assessment of a given community.

CHAPTER 2: LITERATURE REVIEW

2.1 AIR POLLUTION IN EL PASO DEL NORTE REGION

Exposure to airborne pollutants is a severe cause of worldwide concern for the health of the communities that reside within and surrounding major urban centers. Epidemiological studies have shown a relationship between airborne pollutants and respiratory and cardiovascular disease increase in sensitive populations like the elderly and children with pre-existing respiratory disease [15], [16]. Air pollution poses an increased risk to several populations, thus sparking a growing interest in air quality monitoring and assessment. Evidence has indicated that the border regions tends to experience higher levels of airborne particulate matter, mainly PM_{10} and $PM_{2.5}$ [3], [17], [18].

The El Paso Del Norte Region (the Pass of the North) encompasses Texas – New Mexico – Chihuahua region; more importantly, it is the location of two border cities, Cd. Juarez on the south of the Rio Grande and El Paso, Texas, on the opposite side of the river [19]. These sister cities are monitored by different entities, including the City of El Paso, TCEQ, the New Mexico Environment Department (NMED), and the Cd. Juarez Ecology and Civil Protection Department (DGEPC). These departments are responsible for managing several monitoring systems located throughout the region. The criteria air pollutants (as set by the NAAQS; ground-level ozone, lead, carbon monoxide, nitrogen dioxide, sulfur dioxide, and particulate matter) that are mainly monitored are particulate matter (PM), including particles of less than 2.5 μm in aerodynamic diameter ($PM_{2.5}$), and 10 μm for PM_{10}, which have been seen to pose the highest public health risk. Critically, El Paso has also been designated as nonattainment for PM_{10} according to the U.S. National Ambient Air Quality Standards (NAAQS).

The US-Mexico border is vital for cross-border commerce, immigration, and travel. US goods and services trade with Mexico has totaled an estimated 677.3 billion dollars in exports and imports, leading to an increase in air contaminants due to vehicular fleets coming and going from the border [20], [21].

The economic growth in these sister cities has led to higher populations and has a direct impact on an increase in vehicular emissions, with nearly 1,200,000 passenger vehicles crossing through the Bridge of the America's port of entry every month [22], [23]. As a result, transportation, including private and commercial vehicles, became the primary source of local urban pollution, producing oxides, hydrocarbons, carbon monoxide, and other critical contaminants [24]. This issue is aggravated by differing policies between the two countries, allowing older and ill-maintained vehicles to traverse the cities [18].

The North American Free Trade Agreement (NAFTA) allowed trucking to become a significant industry and source of commerce in El Paso and Cd. Juarez, with nearly 50,000 truck crossings every month at the Ysleta port of entry [23]. It has caused an increase in transportation crossing the border, creating more significant queuing times and worsening air quality as large diesel trucks frequently idle for extended periods. In the US, the transportation industry accounts for 27% of greenhouse gases [25]. Railyards and Railroads also play a significant role in commerce within the PdN, moving 32 % of goods within the US; however, they only account for 6% of freight-related greenhouse gas emissions [25].

Besides vehicular emissions from the border, El Paso and Cd. Juarez is home to large-scale polluting facilities such as Vinton Steel LLC, Western Refining Company LCC, the US Dept of the Army, and Boeing Company, to name a few of the point sources in El Paso [26]. Factories, including power plants and other production factories, make up 58% of air pollution annually [27]. Due to the high level of industrial activities, El Paso has been ranked 4th out of 15th mid-size metros and 19th out of more than 300 cities with poor air quality [28].

Global aviation (domestic and international; passenger and freight) account for 1.9% of all greenhouse emissions [29]. Aircraft operations from the El Paso International Airport and Ft. Bliss accounted for 8,110 activities for a given month in 2021, with 52 daily departures, 174,023 enplaning, and 160,438 people deplaning monthly [30]. Passenger growth has continued, with an increase in flight activities, up to a 99.2% of aircraft activities as reported before the COVID-19 pandemic [30].

Fort Bliss is one of the largest military bases in the US, accounting for 1,500 square miles of restricted air space used for military aircraft operations, missile testing, and artillery training. PM emissions generated on base come from many different sources, such as short-term dust from mother vehicle disturbance of the desert floor and military operations such as burn pits, engine idling, aircraft taxing, and munition waste, to name a few [31]. As a result, the US military is a significant contributor to climate change, with 1212 million metric tons of greenhouse gases emitted from 2001-2017 [32].

El Paso is also subjected to high aeolian activities, which decrease air quality over the air shed due to the region's high aridity. The continuous disturbance of anthropogenic land can have dire consequences, such as increased dust deflation and dust emission from vulnerable environments, e.g., arid and semi-arid environments [33], [34]. Furthermore, human activity has disrupted and increased dust emissions from natural sources such as ephemeral lakes, floodplains, and playas [35]. The increase in land use for residential and commercial expansion severely degrades environments, causing an increase in the aeolian process and directly worsening air quality conditions in many parts of the region.

During the winter, atmospheric stagnation is marked by stable air masses and low wind speeds throughout the PdN [3]. In the late fall through winter, the heating and burning of different biomasses, especially in the outskirt regions in El Paso and Cd. Juarez, have been high contributors to overall PM concentrations in the PdN. The overall buildup of pollutants is often a result of the calm conditions, which further worsen during evenings and early mornings due to the formation of radiation inversions [3].

Even though the US-Mexico border creates a physical separation between the two countries, it also highlights significant disparities in living standards between the two cities. These disparities are evident in the different levels of regulation and control of air pollutants for the sister cities. While it is clear that Mexico federal and state agencies are committed to preserving and maintaining air quality within its regions, they lag behind US environmental and regulatory agencies. As a result, the El Paso and Cd. Juarez airshed is impacted by trans-border pollutant

flux[3], [6]. Figure 1 shows The University of Texas at El Paso (UTEP) and Cd. Juarez "Las Colonias" is affected by trans-border air pollutant flux.

Figure 1: Pollutant over El Paso and Cd. Juarez

The rapid growth of El Paso and Cd. Juarez has spurred a need for air quality exposure and monitoring. Due to the differing spatial-temporal trends of pollutants, centralized monitoring stations are insufficient to provide a thorough exposure assessment [36], [37]. The current TCEQ nonattainment status for criteria pollutants has put El Paso in the spotlight, highlighting the need to fill the gaps in monitoring air pollutants.

2.1.1 PARTICULATE MATTER

Exposure to air pollution is estimated to cause millions of deaths yearly; it is now thought that air pollution is on par with deaths caused by other health risks such as an unhealthy diet and smoking [38], [39]. In addition, particulate matter has been the cause of over 800,000 premature deaths globally and is ranked as the 13th leading cause of mortality worldwide [39]–[41]

Particulate matter or particle pollution refers to either solid or liquid droplets suspended in the air [42], [43]. Some particle pollution includes dust, dirt, soot, smoke, and water droplets;

some particles are large enough to be seen with the naked eye, such as smoke in the air, and some are so minuscule it is impossible to see [39], [44]. These particulates comprise acids, organic chemicals, metals, and soils [41], [43]. The most notable PM includes PM_{10} and $PM_{2.5}$.

Particulate matter is clearly defined by its aerodynamic equivalent diameter (AED) [42], [45]. PM_{10} are considered inhalable particles with an aerodynamic diameter of 10 µm and smaller, and $PM_{2.5}$ are considered fine inhalable particles with an aerodynamic diameter of 2.5 µm. Figure 2 shows the size distribution for PM_{10} and $PM_{2.5,}$ and it shows the AED in relation to human hair and a grain of sand where $PM_{2.5}$ is substantially smaller than a strand of hair.

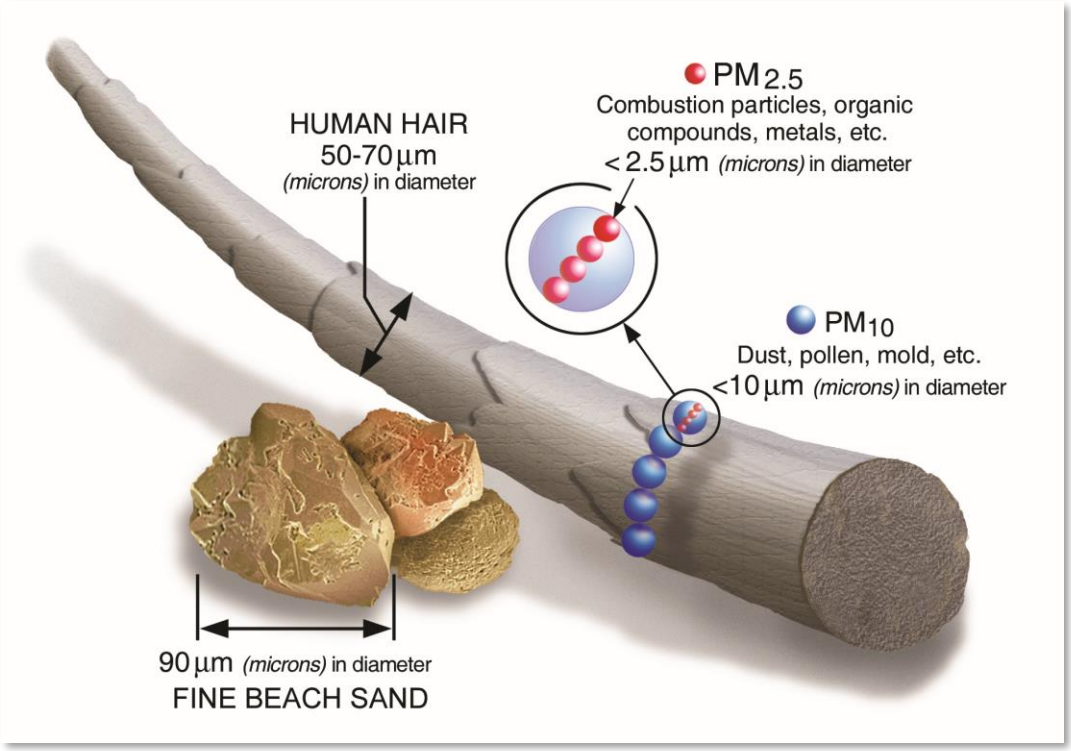

Figure 2: Size Distribution of $PM_{2.5}$ and PM_{10}

Due to its size and proportionality, there are many health concerns regarding the particulate matter. For example, the larger PM_{10} can cause eye, nose, and throat irritation because of its increased size. On the other hand, $PM_{2.5}$ is more dangerous due to its smaller size, as these particulates can deposit into deeper regions of the lungs and diffuse into the bloodstream [46].

Current research has shown increased morbidity and mortality related to PM exposure [7], [47]–[52].

Respiratory deposition is a significant concern for PM, as the hazard is determined based on the chemical composition and site where the particle deposits in the respiratory tract [42]. Respiratory deposition goes through three stages, as explained by [42]. First, deposition happens in the nasopharyngeal region, where the air is inhaled, warmed, and enters the body. Second, the process occurs in the tracheobronchial area, where the particulates continue their path to the bronchioles. Finally, it is diffused into the pulmonary and alveolar regions. Deposited particulates have severe adverse health effects, such as premature death in people with pre-existing lung or heart disease, nonfatal heart attacks, arrhythmia, aggravated asthma, coughing, or difficulty breathing [44]. Apart from health, PM causes several environmental effects, such as visibility impairment, acidification of waterways, nutrient depletion, and habitat destruction.

To control or mitigate the harmful effects of PM, the US EPA has been setting and reviewing standards for PM pollution. The enactment of the Clean Air Act in 1970 required the EPA to set NAAQS for six criteria pollutants where the clean air act has defined primary and secondary standards. Primary standards provide health protection to sensitive populations such as asthmatics, children, and the elderly; the secondary standard protects the public's welfare [53]. Table 1 shows the primary and secondary standards for $PM_{2.5}$ and PM_{10}.

Table 1: NAAQS Table for $PM_{2.5}$ and PM_{10}

Particulate Pollution (PM)	**$PM_{2.5}$**	Primary	1 year	12 µg/m^3	The annual mean averaged over 3 years
		Secondary	1 year	15 µg/m^3	The annual mean averaged over 3 years
		Primary & Secondary	24 hours	35 µg/m^3	98th percentile averaged over 3 years
	PM_{10}	Primary & Secondary	24 hours	150 µg/m^3	Not to be exceeded more than once per year on average over 3 years

The EPA enforces these standards through state implantation plan (SIP) requirements. States are required to control air pollution from emission sources, and each state is required to handle air pollution within its region. The EPA will work with the conditions and designate an area based on the air quality data from monitors and designate an area based on whether it meets the standard. The PdN has not met this criterion for PM_{10} as of 2022 but has been within limits for $PM_{2.5}$. The attainment status for $PM_{2.5}$ and PM_{10} for the El Paso area can be seen in Table 2.

Table 2: El Paso Area: Attainment Status for $PM_{2.5}$ and PM_{10}

PM_{10}	150 µg/m^3	24-hour	Moderate Nonattainment
$PM_{2.5}$	12 µg/m^3 (2012 standard)	Annual	Unclassifiable/Attainment
	15 µg/m^3 (1997 Standard)	Annual	Unclassifiable/Attainment
	35 µg/m^3	24-hour	Unclassifiable/Attainment

2.2 NEAR-ROAD COMMUNITY EXPOSURES

More than 45 million Americans are living, working, or attending school within 300 feet of a major road, airport, or railroad [54], which is known to cause harsh consequences, such as higher rates of asthma, cardiovascular disease, impaired lung development, and premature death in children [38], [41], [54]. In addition, previous literature found a high prevalence of 10-year-old children who live near roads and develop asthma or wheezing [41]. These health risks are a significant concern for Americans living near heavily transited roads.

The Environmental Protection Agency (EPA) has worked tirelessly to reduce vehicular emissions near roadways over the past decades. The EPA has established and implemented stringent emission standards and fuel requirements, reducing emissions from newer cars. The EPA also started the Near-Road (monitoring) network as part of the 2010 NAAQS review [55], leading to more near-road NO_2, CO, and PM data being readily available.

Lal [55] assessed the near-road monitoring network and non-near-road monitoring in the continental US using observational data from 2017 and 2018. It was found that $PM_{2.5}$ concentrations between near-road and non-near-road had a difference of 0.50 $\mu g/m^{3.}$ Furthermore, 61% (44 out of 72 sites) of the near-road sites had a higher 2-year average of $PM_{2.5}$ concentration than non-near-road sites. However, Lal attributed $PM_{2.5}$ variations, regardless of its distance to roads.

It was seen that the near-road sites had a higher $PM_{2.5}$ average than the primary standard of 12 $\mu g/m^3$. It was also found that the annual average daily traffic (AADT) and the Fleet-Equivalent AADT (FE-AADT) had a positive and statistically significant correlation (α= 0.05) for NO_2 and CO, but this was observed as a weaker and not statistically considerable parameter for $PM_{2.5}$.

Traffic-related air pollution (TRAP) can vary spatially and temporally, especially in the PdN. For example, the rapid urbanization and industrialization in El Paso and Cd. Juarez led to a rapid deterioration of air quality. However, due to cost and maintenance, the city does not have

enough federal regulatory monitors, causing inconsistent and incomplete exposure analysis throughout the region. Furthermore, the insufficient emission inventory data from Cd. Juarez limit analysis and exposure assessments; this is especially important due to pollutant flux over the border, affecting both cities

Finally, due to differences in international policy and overall funding, it is challenging to accomplish and enforce air pollution regulations between Mexico and the United States. Creating a demand for affordable monitoring would fill the gaps in conventional tracking by providing a larger spatial-temporal view of a region. This approach would also help develop quicker assessments of criteria pollutants and assist in decision-making when establishing monitoring stations in higher-risk areas.

2.3 LOW-COST SENSORS

Technological advancements have led to the emergence of relatively new technology, low-cost air quality sensors that measure specific air pollutants and other gaseous pollutants. These sensors aim to be user-friendly, compact, and, more importantly, affordable than other regulatory equipment. In addition, these low-cost sensors can provide observations at a high spatial resolution in real-time, offer the opportunity to expand on the limitations of regulatory monitoring stations, and help involve the community with community air monitoring. However, there is concern about the quality of the instrument and reliability of the data being generated.

Air quality in the United States has been measured using strict measures set by the US Environmental Protection Agency through equipment that implements and follows the federal reference methods (FRM) or federal equivalent method (FEM) [56]–[58]. An instrument designated as FRM indicates that it has been developed to a clear and defined standard for a specific pollutant. Furthermore, an instrument commissioned by FRM or FEM has completed rigorous testing and analysis and can be used to monitor for criteria pollutants in compliance with NAAQS standards.

The EPA has continued to evolve in its approach to monitoring ambient air pollution, transitioning from the philosophy of defining methods and reference methods to adding equivalent methods, allowing flexibility in monitoring and the ability to upgrade. Low-cost sensors, in their current state, cannot operate as stand-alone regulatory monitoring stations; however, they can play a vital supporting role when integrated with other monitors. These sensors also offer additional avenues to redefine spatiotemporal characterization at different levels [57].

There is a worldwide upward trend in adopting low-cost sensors, leading to an increase in air quality data collection beyond what is currently provided by federal reference stations. However, low-cost sensors do not operate or obtain the same level of accuracy as other methods, often putting the quality and validity of the sensor's data in question. On the other hand, Snyder et al.[59] described how it is not vital for the sensors to obtain the same level of accuracy as other FRM/FEM monitoring systems. Low-cost sensors should not serve as individual stations alone; instead, they should be used to provide a preliminary analysis of a given area and evaluate current trends within their deployment zone.

Low-cost sensors supplement routine ambient monitoring networks, further enhancing regulatory monitoring and benefiting different sectors. For example, these sensors can help improve source compliance monitoring; sensors can be utilized at the source location or facility, assisting industries in monitoring emissions and improving quality of life [59]. In addition, urban air pollution exposes the public to dangerous toxins, decreasing the quality of life. Therefore, these low-cost sensors provide an avenue for community monitoring, where the public can monitor their exposure.

In conclusion, federal, state, and local agencies must create guidelines for using sensors and interpreting data to prevent data quality and interpretation challenges [59]. Currently, the EPA has created resources and is working to facilitate the use of low-cost sensors.

2.3.1 LOW-COST SENSOR OPERATING CONCERNS

There is no doubt that low-cost sensors enable higher spatial-temporal and spatially dense measurements for PM compared to traditional reference monitoring stations, which have limited spatial and temporal resolution. Low-cost sensors have allowed for more excellent monitoring due to their affordable price compared to a regulatory monitoring station's startup and upkeep costs. They have been widely used in low-middle-income countries and regions with few regulatory monitoring stations. However, the biggest challenge for low-cost sensors is their data's reliability, accuracy, and quality. Users may be alarmed when their low-cost units show higher peaks than regulatory stations. Alternatively, low-cost units can cause a false sense of security with lower values than regulatory stations, driving users to believe that their air quality is of better quality when it is not.

Most commercially available low-cost PM sensors use light-scattering as their principal mechanism [60]. Light scattering in these sensors functions primarily off the Rayleigh, Mie, or geometric scattering [60]–[63]. Where the Rayleigh scattering technique refers to the scattering of light off of air molecules, the Mie scattering is the scattering of electromagnetic waves by a spherical medium [42], [45], [62], [64]. Like other low-cost sensors, PurpleAir sensors use light scattering and do not measure individual particle scattering, but the overall scattering of the particles at a given volume [60].

Low-cost sensors are calibrated before being delivered by the manufacturer. Sensor calibration is relatively easy. The US EPA recommends collocation for low-cost units. Collocation is where the low-cost sensor is deployed next to a regulatory monitor (FRM/FEM), and they are operated over a specific set of time. Thus, the regulatory monitor and low-cost sensor are exposed to the same environmental conditions. This period of collocation is essential to determine the accuracy and validity of the low-cost sensor.

Many environmental factors can affect the accuracy of these sensors. The US EPA recommends considering the seasonal trends of the pollutant that will be measured. Extreme

temperatures and relative humidity can also affect sensor readings [65]–[67]. Once the data has been collected, it is reviewed for outliers, expected patterns, interferences, and drift or shift. At this point, the information is then compared to the regulatory station. The US EPA suggests comparing the data by plotting a correlation graph and looking at the R^2 value to determine the agreement between the low-cost sensor and regulatory monitor.

The particle size distribution and chemical composition are well-known for low-cost sensors, especially in PA-II devices [68]. However, the most recent research on the PA-II sensor and low-cost sensors using light scattering as their primary operating system shows that relative humidity can alter the hygroscopicity of aerosols, affecting light scattering and creating a bias within the sensor [66], [68]. As such, the low-cost sensors are highly subjective to environmental factors and can cause discrepancies in data. In addition, further concerns arise over the long-term use and life of the device.

2.3.2 LOW-COST SENSOR PERFORMANCE

Low-cost sensors have become widely popular and have caused a paradigm shift away from traditional air pollutant monitoring stations. As a result, many review articles have addressed low-cost sensors for use in traditional air quality monitoring, focusing on an emerging technology or providing an overview of low-cost sensors' applications. In response, many studies have questioned the validity of the data quality provided by these sensors; however, a universal solution for sensor data quality has not been provided due to the variability in sensors and use.

It is vital to understand the main goals of the field sensor's data validation to understand its overall performance and the effect on data quality. The data validation goals are to compare inter-sensor differences, validate the consistency of high exposure readings, compare concentrations from the low-cost sensor to other higher-grade instruments, and estimate particle mass conversion coefficients to be various indoor and outdoor indoor microenvironments [69].

Furthermore, understanding the operating ranges and abilities of the sensor gives an overview of the sensor's performance over time.

Moreover, low-cost sensors are also susceptible to environmental conditions, where different environmental settings and pollutant attributes could affect the R^2 between low-cost sensors and reference stations [70]. Wang [71] studied the effect of environmental factors on low-cost sensors by using an environmental chamber to examine the environmental factors that have the most effect on the sensors. Temperature was found to have a minimal impact on the sensor's performance as opposed to relative humidity (RH) because, theoretically, light scattering and absorption are independent of temperature [64], [71]. While RH and the particle composition had a high impact on the sensors, this was likely due to RH affecting particle size, as demonstrated when levels of RH were increased from 20% to 90%. Other studies have found that different particles, such as saline spray or cigarette smoke, significantly affect light scattering. However, there is not enough information to conclude how different particles from arid environments, coal dust, or road emissions affect a sensor's viability and performance [72]–[75].

Field conditions can pose discrepancies and produce varying results, leading to unpredictability in the sensor's data and the inability to recreate specific scenarios for data quality assurance [76]. In a study by Tryner [76] evaluated the low-cost sensor developed by PurpleAir in a laboratory setting. $PM_{2.5}$ mass concentrations from the low-cost sensor were compared with those of a tapered element oscillating microbalance (TEOM) in an aerosol chamber. This comparison created a calibration equation that could be utilized when the sensors were deployed in an environmental setting. Tryner [76] used the National Institute of Standards and Technology (NIST) urban PM concentration to compare the values recorded by the TEOM and PA-II-SD. It was found that the channels "$PM_{2.5}$ CF =1" and "$PM_{2.5}$ ATM" at concentrations below 30 $\mu g/m^3$ values were equal to the TEOM.

In contrast, concentrations higher than 30 $\mu g/m^3$ where "$PM_{2.5}$ CF =1" did not increase linearly with the concentrations recorded by the TEOM. The PurpleAir sensors tended to underestimate the concentrations reported by the TEOM. The results of the study suggested that

the aerosol used to calibrate the PurpleAir devices is like that of the NIST Urban PM; however, this can cause discrepancies in real-world applications, where PM may not be of the same geometric mean (0.0042 µg), and a geometric standard (2.05).

In contrast, many other studies have shown how PurpleAir sensors tend to overestimate concentrations compared to other federal monitoring sites [77]–[80]. A year and 4 months of data were collected in an in-depth sensor evaluation conducted by Magi et al. (2020) in the humid city of Charlotte, North Carolina. This evaluation had sensors located next to the outlet of a Beta Attenuation Mass 1022 (BAM-1022) monitor, which was maintained and regulated by the Mecklenburg County Air Quality (MCAQ). Magi utilized a multiple regression model to increase the accuracy of the low-cost sensor compared to the reference monitor. The sensors were directly affected by RH due to the hygroscopicity of the aerosol and refractive index on $PM_{2.5}$. RH affected the sensor more than any other parameter, causing an increase of 27-57% in data accuracy. When the multiple linear regression model (MLR) was applied to the raw data, it is essential to note that the higher percentage of improvements was for moderate to high RH.

Different environments will expose the sensors to different meteorological conditions, and such differences in operation and accuracy are expected. For example, as shown above, RH will play a significant role in the instrument's accuracy in high-humidity climates and should be considered for climates with moderate to high RH. Furthermore, since RH and, at times, temperature (T) plays a role in the accuracy of the data, RH will define the instrument’s accuracy while deployed.

Low-cost sensors have been shown to perform relatively similarly to each other; however, as noted before, climatic changes will affect the sensor’s accuracy [59], [81]–[83]. A study [72] evaluated the performance of a low-cost sensor network in the Los Angeles area. Los Angeles has an entirely different climate from North Carolina. Los Angeles's dry Mediterranean climate is primarily mild to hot year-round [84]. The assessment was conducted over two weeks for 46 different sites, one in the summer of 2019 and one in the winter of 2020. The raw sensor performance for the two study periods underestimated the Los Angeles County average by 9.4

$\mu g/m^3$ and 12.7 $\mu g/m^3$, respectively. It is important to note that Liu et al. did minimal data correction, only using hourly data provided by PurpleAir and filtering out data that was out of the manufacturer's parameters.

Furthermore, another study [83] showed that relative humidity adversely affected sensor performance compared to a reference station. If the sensor was exposed to high RH (RH>75%), the sensor tended to overestimate PM values; however, if the sensor was exposed to low levels of RH (RH < 50%), the sensor tended to underestimate PM concentrations. During low ambient humidity, the sensor also deviated considerably from the $PM_{2.5}$ reference value. It is also important to note that the study underestimated sensors exposed to high humidity, which could be caused by an obstruction with the sensor's enclosure. The study also showed differing levels of R^2 when sensors were compared to reference stations for hourly averages, with them being 0.47-0.86 for continuous monitoring of $PM_{2.5}$ and 0.24-0.56 for continuous monitoring of PM_{10}.

Most studies have concluded that the low-cost sensor cannot perform to the level of other monitors but can still be a viable tool integrated with other regulatory monitoring [85]–[87]. The sensor's performance seems to be affected by RH due to the device's light-scattering sensors, which has been seen in many other studies [76], [88]–[90]. However, research varies regarding the accuracy of the data, where sensors tend to underestimate or overestimate when compared to regulatory monitors. In addition, most sensors had a form of calibration or correction to align the data better. Additional studies that show the type of sensor and correction can be seen in Table 3, which shows previous research done on low-cost sensors and their functionality

Table 3: Research on Low-Cost Sensors

Sensor (Make/ Model)	Topics												Study	Major Findings
	Calib.		FRM/ FEM	MC		OPE	Aerosol			Sensor Properties		Correction Methods		
	IF	IL		Temp	RH		Conc	Size, Density, Comp	Dist	IC	IS			
PA-II- SD PurpleAir Sensor	x		x		x	x			x			Geographically Weighted Regression (GWR)	[91]	The GWR reduced the sensor bias and residual errors by 36%. Sensor bias was caused by high temp, humidity, and operating time.
DC 1700 Dylos Corp			x	x				x				Linear Regression and Residual Kriging	[92]	Kriging improved the R^2 from 0.05 to 0.31, 0.57 to 0.62, and 0.77 to 0.92 at Westmorland, Seeley, and Holtville, respectively.
PA-II- SD PurpleAir Sensor				x	x	x		x	x			None: Raw Data was used	[93]	$PM_{2.5}$ values were low 5 and moderate 25; the sensor had a bias of 35% for 24hr mean PM value

KOALA Monitor (Plantower Sensor)			x	x	x		x	x	x	x	x	Linear Regression	[12]	R^2 was good at three sites being >0.83, while one site was 0.44 after adjustment.
SDS0111 v1.3	x	x	x	x	x	x				x	x	Correlation Analysis and normalized root-mean-squared-error	[83]	Correlation analysis showed that sensors overestimated PM in high RH (>75%) and underestimated when RH <50%. R^2 with reference station was 0.63-0.87 for continuous monitoring and 0.69-0.93 for lab testing.
AirBeam	x		x	x	x							Linear Regression (LR), Random Forest (RF), and Stacked Ensemble (SE)	[94]	The applied LR, RF, and SE resulted in R^2 values of 0.63,0.73, and 0.80, respectively.
Plantower PMS1003	x	x		x	x	x	x	x				No correction methods	[95]	Sensors are affected by humidity at levels <50 % humidity, and at this point, it was impossible to create an appropriate correction factor.

PA-II- SD PurpleAir Sensor	x		x	x	x	x		x		x	x	Multiple Variable Regression, Deployment Records, and Fifth Percentiles	[96]	High R^2 between sensors inter-channel and inter-sensor, when compared to an FRM site, was reported to have an R = 0.76, MAE = 2.9 µg/m^3, and a bias of -0.5 µg/m^3.
Canary-S models (Plantower Sensor)	x		x	x	x		x		x			Random Forest Regression (RF)	[88]	Raw data against FRM R^2 = 0.73 after correction R^2 = 0.81.
Bare Sensors and Integrated Devices		x		x	x	x		x				Linear Regression	[13]	RH accounted for 11% of the variability and plays a significant role in sensor performance, while temperature has no significant effect on sensor performance.
LILI-1 Platform	x		x	x								Alphasense Correction (AAN 803-01)	[97]	Sensors showed high relative errors if there was a high RH; the field calibration yielded an R^2 value of 0.8 for PM_{10} and $PM_{2.5}$.

SPS30 (Sensirion) sensor	x		x	x	x	x						Machine Learning: Geographical Random Forest (GRF) and Air Variational Graph Autoencoder (AVGAE) model	[98]	Model prediction for $PM_{2.5}$ had an R^2 of 0.68-0.75; the GRF produced better accuracy than the AVGAE model.
PA-II- SD PurpleAir Sensor			x	x	x	x	x	x	x	x	x	Linear Regression	[99]	Sensors were highly spatially correlated r>0.86, and indoor sensors performed more reliably than outdoor sensors.
OPC N2 and PM Nova Sensor	x	x		x	x			x				Linear Regression	[100]	The OPC N2 and Nova can record PM with good accuracy with linear regression with GRIMM (OPC N2, R^2 = 0.954-0.987 and PM NOVA, R^2= 0.872-0.981). There was a better performance for $PM_{1-2.5}$ than PM_{10}.

Legend:

Calib: Calibration

IF: In-field

IL: In-laboratory

MC: Meteorological Conditions

OPE: Optical Property Effects

Conc: Concentration

Comp: Composition

Dist: Distribution

IC: Interchannel

IS: Intersensor

2.3.3 LOW-COST SENSOR CALIBRATION TECHNIQUES

Low-cost sensors can fill in monitoring gaps and improve spatial and temporal data. However, low-cost sensor data is unreliable and lacking in accuracy compared to federal monitoring stations. Furthermore, the sensors are susceptible to environmental conditions such as temperature and humidity, further comprising the quality and accuracy of the data. As a result, many research institutions and government agencies have sought calibration equations or general calibration techniques to bring the low-cost sensors closer to monitoring stations.

For example, the US EPA recommends that users make a “side-by-side” comparison of the low-cost sensor and a regulatory monitoring station. In the comparison process, the low-cost sensor is collocated next to a regulatory station for 7-14 days, where both the low-cost sensor and the monitors are in “real-world” conditions [101]. The data is then compared to the regulatory monitor to create the calibration formulas; however, many researchers have taken different approaches to this process with varying levels of success.

The PA-II-SD sensor utilizes a Plantower PMS (models 1003 through 7003), a dual laser dust sensor that uses light scattering to measure the value of suspended particles in the air. These Plantower sensors report the size distribution of particles from 0.3-10 μm in 6 bins and the size distribution in the unit number of concentration and the mass concentrations of PM_1, $PM_{2.5}$, and PM_{10}[102]. In addition, PurpleAir follows a correction factor for reporting PM data to its servers.

The correction factor (cf) for the PurpleAir $PM_{2.5}$ sensor has been developed with the help of the US EPA. The developed correction factor utilized a US-wide dataset where state, local, and tribal agencies received data from PurpleAir sensors across the country. PurpleAir provides users with two corrections: "cf = atm” and “cf = 1.” The PurpleAir correction for “cf = 1” has different selection criteria where $R^2 = 0.65$ and $R^2 = 0.64$ for “cf = 1” and “cf = atm,” respectively. "cf = atm" is used for sensors located outdoors, and "cf = 1" is used for indoors.

The US EPA looked at many variables for the PurpleAir correction equation. The development of the equation looked at many variables such as $PM_{2.5}$, binned counts ($B_{>0.3'}$, $B_{>0.5'}$,

$B_{>1.0'}$, $B_{>2.5'}$, $B_{>5.0'}$, $B_{>10.0'}$), temperature, RH, and dewpoint (D). The original iteration of this study can be seen in Equation 1, where b represents the slope of the PurpleAir $PM_{2.5}$ and Federal Methods (FM) $PM_{2.5,}$ and s represents the sensor being used [103].

$$PA_{cf_1} = s_1(PM_{2.5}) + b \quad (1)$$

This formula was applied to create a better linear fit between an FRM/FEM station and the sensor leading to an R^2 of 0.78. It was found that RH was the environmental parameter that most influenced the correlation between the stations, raising the R^2 from 0.78 to 0.831. The formula was then changed to include RH and "i," which represents a constant value; Equation 2 is as follows.

$$PA_{cf_1} = s_1(PM_{2.5}) + s_2(RH) + i \quad (2)$$

However, RH and temperature were found to improve the R^2 from 0.831 to 0.832, which is a higher increase than just using RH alone; the equation is as follows.

$$PA = s_1(PM_{2.5}) + s_2(RH) + s_3(T) + (i) \quad (3)$$

The temperature, relative humidity, and $PM_{2.5}$ are significantly correlated; thus, a new approach was used to multiply these factors rather than adding the parameters. As before, the R^2 significantly changed when using RH and T, then just using RH. The new variation changed the R^2 from 0.832 to 0.836 and 0.838 using only RH and RH and T, respectively. The new Equations 4-5 are shown below.

$$PA = s_1(PM_{2.5}) + s_2(RH) + s_3(RH)(PM_{2.5}) + i \quad (4)$$

$$PA = s_1(PM_{2.5}) + s_2(RH) + s_3(T) + s_4(PM_{2.5})(RH) + s_5(PM_{2.5})(T) + s_6(RH)(T) + s_7(PM_{2.5})(RH)(T) + i \quad (5)$$

In the development of the US-wide correction, mean bias error (MBE) and mean absolute error (MAE) were considered. The US-wide correction model was selected because it was less complex and less likely to overfit the data; it primarily relies on root-mean-square-deviation (RMSE) and spearman correlation because they have similar trends to that of MBE and RMSE. The US-wide correction can be seen below in Equation 6; AB represents the hourly mean between the channel a and b two-minute data.

$$PM_{2.5_c} = 0.52\,[PA_{cf_1}\,(\bar{x}(AB)] - 0.085(RH) + 5.71 \quad (6)$$

This correction equation was developed to improve sensor performance across the US; the correction factors' limited complexity helps broaden the conditions and allow for broader adaptation from other US-based sensors. However, this calibration equation is unable to address other issues that are present in PurpleAir devices, such as failures caused by channels A and B (channel noise, significant jump in channel data, error in RH or T), sensor drift due to age, and sensor lifespan in ambient conditions. Nevertheless, it is essential to note that the data has become more accurate through the nationwide cf, even during harsh conditions such as wildfires.

Linear regression is used for FRM and FEM quality assurance in much of the literature regarding PurpleAir devices, where linear regression calculates a slope, intercept, and correlation [104]. In a study by Barkjohn [104], they applied the US-wide correction for $PM_{2.5}$ in 16 states across the United States. It was found that under typical ambient conditions, the raw data produced by PurpleAir sensors overestimated $PM_{2.5}$ concentrations by 40%. Barkjohn utilized a simple linear regression and found that it reduced much of the bias produced by the raw sensor and improved the RMSE and MBE in all regions except for Alaska. After applying the RH term to the regression, it was found that the bias was further improved, except in the southeast, where the bias

increased by <10%. It is important to note that Alaska's harsh temperatures could be attributed to the sensor's increase in bias. The Alaskan temperatures are out of operating conditions for Plantower sensors; however, this was not seen in other sensors that also experienced sub-freezing temperatures (about 6% of the US dataset), suggesting unique particle properties for PM in Alaska.

The multiple regression conducted by Badura's study showed notable differences in data quality. The multiple regression with the addition of the RH and T to the equation had a more significant impact, showing an improvement in the goodness of fit. The R^2 value increased by 0.02, from 0.87 to 0.89, and the RMSE error decreased to 4.2 μg/m^3 from 4.5 μg/m^3.

Similar effects were also seen in a study by Romero et al. (2020), which looked at developing a multiple regression model to calibrate low-cost sensors using reference monitors. The study utilized a PurpleAir sensor located next to the "Campo de Marte Air Quality Station (AQSMarte)" over three weeks [105]. The model used a multivariate regression utilizing the PM and meteorological data; the multivariate regression equation can be seen below.

$$Y_i = \beta_1(X_i) + \beta_2(T) + \beta_3(RH) + \beta_0 \quad (7)$$

Y_i corresponds to the reference station PM, and X_i represents the PM sensor's measurement. The model's beta coefficient values can be seen in Table 4 $PM_{2.5}$ had a value <1.00, RH had a value of 1.027, and the temperature had a value of 0.119. This model showed a highly positive correlation with the reference monitor for $PM_{2.5,}$ with an R^2 of 0.8 [105].

Table 4: Multiple Regression PurpleAir Sensors Model Values of Betas

Multiple Regression $PM_{2.5}$	**β_1**	**β_2**	**β_3**	**β_0**
$PM_{2.5}$	0.704	1.027	0.119	-21.517

The model showed temperature as the most influential meteorological parameter when, typically, RH has shown to be an integral part of particle size distribution. The study also

demonstrates that the measurement for $PM_{2.5}$ and PM_{10} have decent performance but have lower performance and accuracy for temperature and RH.

Many studies have been conducted to bring low-cost sensors more in line with regulatory monitors. The EPA has funded and increased research efforts in developing sensor calibration. It has been found that a univariate or multivariate regression can reduce RMSE and BME and reduce sensor bias, leading to a higher level of accuracy when compared to FRM/FEM monitors. More research efforts are being led to use neural networks and artificial intelligence to create better models and calibrations for low-cost sensors [65], [89], [94], [106], [107].

CHAPTER 3 STUDY DESIGN

3.1. SCIENTIFIC APPROACH

Recent upcoming low-cost sensor technology has made them readily accessible and affordable for the general public; as such, there has been a growing interest in the performance and quality of the devices. Furthermore, low-cost sensors can assess air quality in underserved regions and be deployed in mass, providing more spatially rich data than reference stations. However, the quality of data generated by these low-cost sensors has been highly debated, sparking an interest in the research community to evaluate the efficacy of the sensors. This thesis looks to assess the quality of the data generated by the low-cost sensors and look at further applications of the data generated by the instruments once it has been cleaned and corrected.

Quantitative data was gathered from the low-cost sensors and TCEQ CAMS, and the data collected from CAMS was utilized to find a correction factor for the low-cost sensor data. The low-cost sensor data was also utilized to create a land-use regression model to identify the variability of PM when close to different variables. It is essential to note the limitations of this study; data gathered from this study happened during two different seasons, which could cause differences in collocated deployment, where correction factors gathered during the cold months might not be as accurate as the data gathered during the hotter months. Furthermore, the amount of data collected and the time when the data was collected might not be enough to summarize the air quality in the shared air basin.

The sensors were deployed in sites with differing annual average daily traffic (AADT) in El Paso and Cd. Juarez, where Cd. Juarez had a stronger focus on deploying sensors in industrial sectors, and El Paso deployed sensors within the community at several public schools within the El Paso Independent District (EPISD). Data was gathered periodically during the two-month study period; this data was corrected using previous data collected from two weeks when the sensors were collocated next to a CAMS station during the cold months. In addition, sensors were regularly assessed, and faulty sensors were replaced with spare units, which were also corrected using data

from their two-week deployment with the CAMS station. Once the data was corrected and assessed, it was used to develop a land-use regression model, using the different PM concentrations from the sites and comparing them with different environmental and human markers within the region. In conclusion, this project is a case study on the air quality data generated by low-cost sensors and how this data can be corrected and used in modeling to forecast hotspots in the region.

3.2. SELECTION OF THE SITE LOCATION

Vehicles significantly contribute to air pollutant emissions, posing a risk for individuals living, working, or going to school near busy roadways [108]—This project utilized low-cost sensors to evaluate air pollution at different sites in El Paso and Cd. Juarez and areas surrounding Dona Ana County, site locations varied between El Paso and Cd. Juarez. El Paso sites were selected based on the community exposure to traffic-related vehicular emissions, where exposure varies from sites with high and low vehicular traffic (within a 500 m zone). Furthermore, El Paso sites were selected to be placed in elementary schools due to their varying levels of AADT (low and high), and schools were the best platform to integrate the community. Sites in Cd. Juarez was selected to be placed in various industrial sectors due to the sheer number of factories (>300) in Cd. Juarez and their effects on air quality [109], [110]. In addition, Cd. Juarez sites were also selected considering their high and low-traffic zones within the industrial districts.

3.2.1 LOW-COST NETWORK EXPERIMENTAL DESIGN IN EL PASO DEL NORTE

Low-Cost sensors were deployed and installed at 32 critical El Paso and Cd locations. Juarez due to their AADT and conditions. There are 12 locations with dual sensors. $PM_{2.5}$ was monitored at 17 elementary schools with high and low AADT, 12 schools are in El Paso, and the remaining 5 are in Cd. Juarez. Cd. Juarez hosted 14 sites in industrial regions where the sampling took place over two months, from March through April 2021. The sensor's placement through El Paso and Cd. Juarez can be seen in Figure 3, where most sensors are located next to a primary

road. Figure 4 shows the road layout in the PdN; El Paso has a well-defined infrastructure and Cd. Juarez has a menagerie of primary, secondary, and tertiary roads. Table 5 displays information about each location, including the number of sensors on the site, their AADT classification, and the site's classification (Elementary site, industrial site, or calibration site).

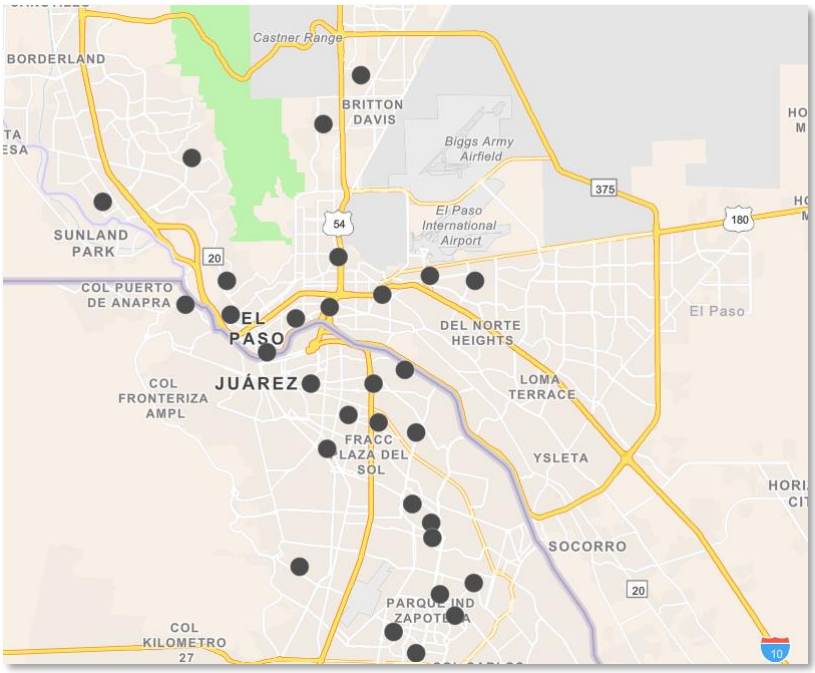

Figure 3: Low-Cost Sensors Location in El Paso del Norte

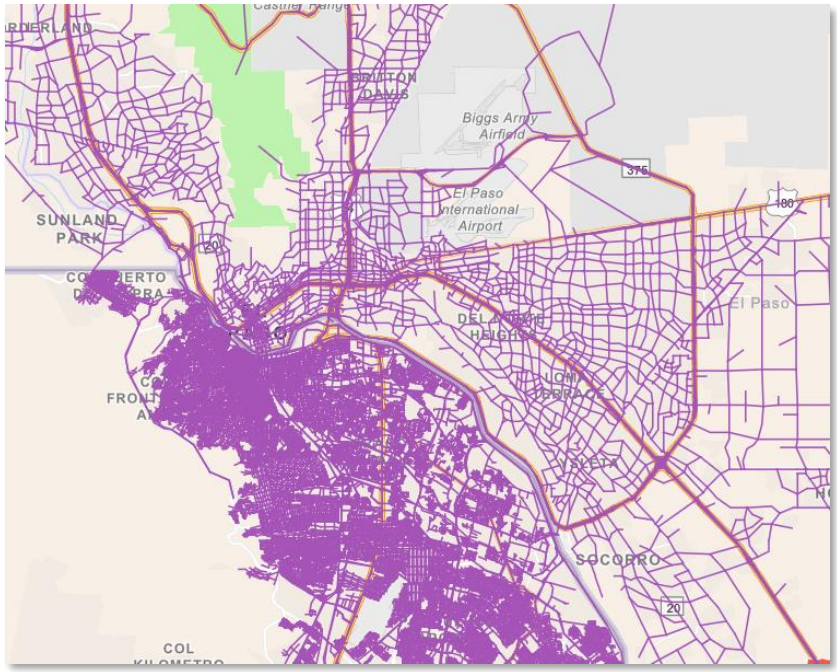

Figure 4: Roads in El Paso del Norte

Table 5: PurpleAir Name of Site and Sensor

Name on PurpleAir Website	Latitude	Longitude	AADT	Type of Site
Zavala	31.7718	-106.4470	High	Elementary School
Zavala 2				
Hawkins	31.7774	-106.4185	High	Elementary School
Bonham	31.7866	-106.3922	High	Elementary School
Douglass	31.7663	-106.4657	High	Elementary School
Coldwell	31.7951	-106.4424	High	Elementary School
Aoy	31.7508	-106.4815	High	Elementary School
Aoy 2				
Mesita	31.7839	-106.5037	High	Elementary School
Cielo Vista	31.7840	-106.3676	Low	Elementary School
Park	31.8567	-106.4507	Low	Elementary School
Park 2				
Whitaker	31.8509	-106.4254	Low	Elementary School
Western Hills	31.8415	-106.5225	Low	Elementary School
Zach White	31.8208	-106.5713	Low	Elementary School
UACJ-PAC07	31.7383	-106.4311	High	Elementary School
UACJ-PAC12	31.7210	-106.5218	Low	Elementary School
UACJ-PAC13	31.7033	-106.4273	High	Elementary School
UACJ-PAC16	31.6846	-106.4516	High	Elementary School
UACJ-PAC11	31.6577	-106.4524	High	Elementary School
UTEP 1	31.7687	-106.5012	High	Calibration Site
UTEP 2				
UTEP 3				
UACJ-PAC08	31.7271	-106.3830	High	Industrial Sector
UACJ-PAC09	31.7182	-106.4204	Low	Industrial Sector
UACJ-PAC01	31.6162	-106.4103	Low	Industrial Sector
UACJ-PAC10				
UACJ-PAC22	31.7154	-106.3979	High	Industrial Sector
UACJ-PAC21				
UACJ-PAC20	31.7363	-106.4238	High	Industrial Sector
UACJ-PAC19				
UACJ-PAC15	31.6576	-106.3995	Low	Industrial Sector
UACJ-PAC04	31.6748	-106.3866	High	Industrial Sector
UACJ-PAC23	31.6067	-106.3994	High	Industrial Sector
UACJ-PAC24				
UACJ-PAC14	31.6878	-106.4015	Low	Industrial Sector
UACJ-PAC02	31.6285	-106.3770	Low	Industrial Sector
UACJ-PAC03				
UACJ-PAC17	31.7355	-106.4616	Low	Industrial Sector
UACJ-PAC18				
UACJ-PAC05	31.7716	-106.5573	Low	Industrial Sector
UACJ-PAC06				
UACJ-PAC26	31.6662	-106.3912	High	Industrial Sector
UACJ-PAC25				
UACJ01	31.7433	-106.4315	High	Industrial Sector

3.3. SELECTION OF LOW-COST SENSORS

PurpleAir Inc makes the low-cost sensor selected in this study. The sensors model is a PurpleAir (PA)- II outdoor air quality monitor equipped with dual laser particle counters (PMS-5003), as well as pressure, temperature, and humidity sensors (BME280 or BME688), ESP8266, and an Arduino board. The sensor's components and exterior can be seen in Figure 5.

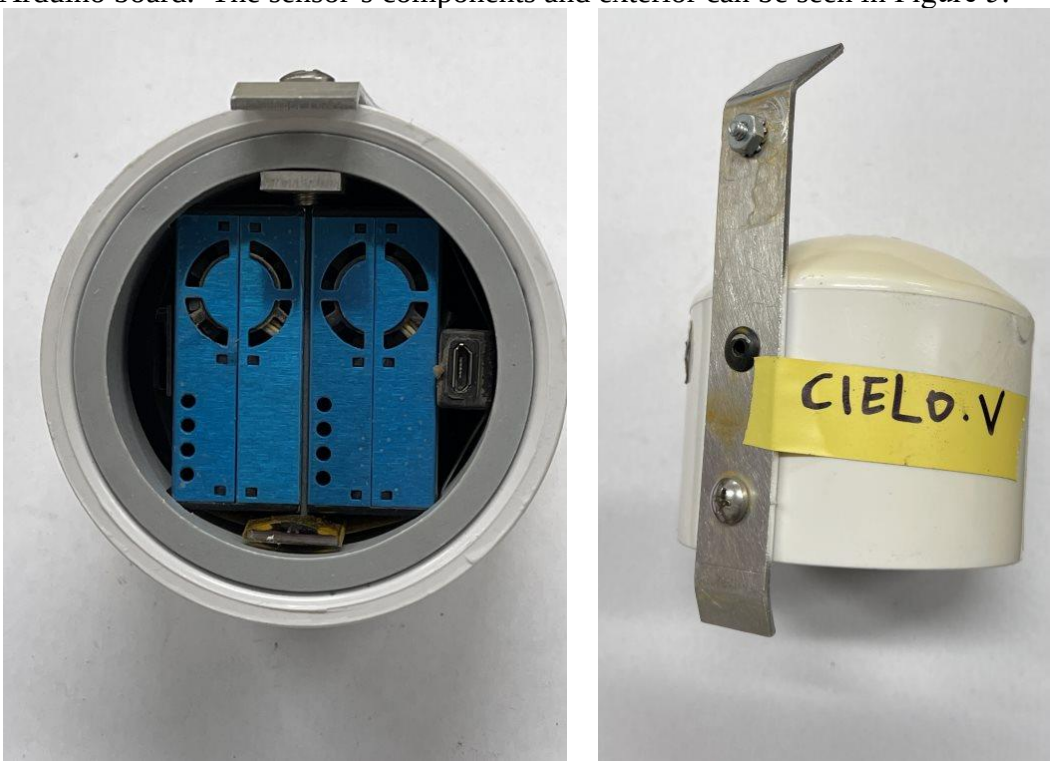

Figure 5: PA-II-SD internal components and external view

The PMS5003 is the 5th generation sensor of the PMSx003 series, developed and manufactured by Plantower. This sensor uses a laser scattering principle to obtain the curve of scattering light change with time. The sensor produces particles binned in different diameters, leaving a unit per volume. The sensor processing was developed using the Mie scattering theory [111], a mathematical-physical theory of particles being scattered over an electromagnetic wave by spherical particles [112], [113]. The sensor data output is returned for each particle having a different size per unit volume of 0.1L and the mass concentration µg/m^3.

The BME280 is a temperature, humidity, and pressure sensor developed for various mobile applications by BOSCH. PurpleAir also utilizes the BME688, a gas sensor with Artificial Intelligence (AI) used to collect temperature, humidity, and pressure developed by BOSCH. Both the BME280 and BME688 have the same features, but the BME688 has a gas scanner, detecting volatile organic compounds (VOCs) and other gases such as carbon monoxide and hydrogen.

The Arduino UNO and the NodeMCU are microcontrollers used by PurpleAir for their microprocessors. These microcontrollers control the functions of the other sensor components by interpreting the results produced by the PA-II components and uploading the data to PurpleAir servers in real-time.

The sensor was selected using the South Coast Air Quality Sensor Performance Evaluation Center (AQMD's) air quality specification (AQ-SPEC), a program that aims to test low-cost sensors and establish performance standards for each sensor being evaluated. The sensors are evaluated by collocating them next to a monitoring station using FRM, FEM, or the best available technology (BAT). The field operations are conducted during a specific 30 to 60-day period. At the same time, laboratory testing is conducted in the AQ-SPEC's laboratories [114].

The PurpleAir low-cost sensor was selected for its high linearity with federal monitoring stations and in-lab testing. As shown in Table 6, the sensor had a high coefficient of determination (R^2) for in-field testing, having a high of 0.98 and 0.97 for $PM_{1.0}$ and $PM_{2.5,}$ respectively; however, the sensor had a mid-range R^2 for PM_{10}. The sensors in lab testing showed high linearity, with most R^2 being between 0.95 and 0.99 for $PM_{1.0}$, $PM_{2.5}$, and PM_{10}.

Table 6: Purple Air Sensor Evaluation By AQ-SPEC's Laboratories

Sensor	Cost	Model	Pollutant	Field R^2	Lab R^2
Purple Air	**$ 259**	**PA-II**	$PM_{1.0}$	0.96-0.98	0.99
			$PM_{2.5}$	0.93-0.97	0.99
			PM_{10}	0.66-0.70	0.95

Furthermore, the sensor's capabilities and ease of use allow for better community integration. PurpleAir's website, as seen in Figure 1, has easy user interference and allows for a preliminary view of the data. The sensor data is uploaded to various PurpleAir servers in real-time. The data can be uploaded via their website or recalled through their JavaScript Object Notation (JSON) application programming interface (API).

3.4. LOW-COST SENSORS DATA COLLECTION

Data was collected from a low-cost monitoring network of 48 PurpleAir PA-II-SD sensors located at 32 El Paso and Cd. Juarez sites. The PurpleAir sensors alternate each laser counter with 5-second readings that average over 120 seconds [115]. The data is then transmitted to the PurpleAir website servers, and the data is also stored locally in the device's internal memory or secure digital (SD) card. The sensor also provides real-time data to a JSON and is available using their integrated API.

The data uploaded to the servers includes $PM_{2.5}$ concentrations, PM_{10} concentrations, temperature, humidity, and relative pressure. The JSON format is essential as it allows for a streamlined download and retrieval of data, and the JSON allows data to be transferred from the server directly to the client. In addition, PurpleAir data is stored in the "ThingSpeak" servers, which allow for retrieval using API and computer languages.

The data is called using an R script which can streamline data calling from multiple sensors by downloading all 48 sensors simultaneously. Furthermore, the downloaded data was retrieved in its original 120 seconds with no other data adulteration. The data was downloaded directly from

the PurpleAir JSON, where the script would format and transmit the data into a readable form in a comma-separated value file (CSV). The data was adjusted to match the region's time zone, going from UTC to MST.

The collected data underwent a preliminary enhancement to help it be processed and compared to a central monitoring station. In addition, the data was enhanced with geospatial markers, which gives the data points a location in time. The markers allow for comparison to nearby monitoring stations. Even though an approximation of the contaminants' concentrations in real-time is sought after, these sensors cannot be used as federally referenced instruments. In addition, the PurpleAir website provides unaveraged and averaged data; however, it is essential to note that this data does not undergo any quality control and represent the average of that hour regardless of the number of data points within that hour, due to this it is assumed that the PurpleAir data from the website may contain errors.

3.5. LOW-COST SENSOR DATA VALIDATION

PurpleAir Inc provides users with a comprehensive list of specific operating parameters for the PA-II-SD sensor, as seen in Table 7; this includes the four criteria parameters that PurpleAir's low-cost sensors monitor for ($PM_{2.5}$, temperature, and humidity.)

Table 7: Operating Range PurpleAir-II

Parameter	Operation Range
Effective Range ($PM_{2.5}$ standard)	0 to 500 $\mu g/m^3$
Maximum Range ($PM_{2.5}$ standard)	$\geq$1,000 $\mu g/m^3$
Temperature Range	-40 °F to 185 °F (-40°C to 85°C)
Humidity	Response time (τ63%): 1 s Accuracy tolerance: ±3% RH. Hysteresis: $\leq$ 2% RH

The data download via the JSON and PurpleAir website undergo a preliminary cleaning to ensure that these operating guidelines are followed. First, the collected data is cleaned, and values outside the specification are disregarded from the dataset. For example, the data point will be

invalidated if a $PM_{2.5}$ value is negative or above >1000. After being "cleaned" to ensure the data is within the instrument's capacity, the remaining data undergo a more stringent procedure.

This data validation procedure is more stringent than what is conducted by PurpleAir, as PurpleAir produces an hourly average regardless of the quality and quantity of data available for the given hour. A $PM_{2.5}$ column is created by averaging the A and B channel base means. Then, data is validated using these criteria:

- The minimum count is < 20 data points per hour
- Data is invalidated if the A/B hourly difference is >5
- Data is invalidated if the A/B hourly percent difference is >70%
- Data is invalidated if the A/B hourly data recovery is <90%.

The low-cost sensors were deployed across El Paso and Cd. Juarez over two months, from March 1st until April 30th, 2021. During this time, the sensors were exposed to real-world conditions, where conditions varied depending on the site. As seen in Table 8, most sensors had a percentage of data invalidation between 6-15 %; however, some sensors experienced higher levels of degradation while deployed and had over 50% of their data invalidated.

Table 8: Low-Cost Sensor Number of online and invalidated hours during the study period

Sensor	Online Hours	Invalidated Hours	Invalidated Hours %
UTEP1	822	56	6.8
UTEP 3	1327	379	28.6
UTEP 2	1327	104	7.8
Cielo Vista	1436	96	6.7
Douglass	1439	122	8.5
Mesita	1435	104	7.2
Park 2	851	55	6.5
Park	1439	211	14.7
Bonham	1426	390	27.3
WesternHills	1312	357	27.2
Whitetaker	1257	370	29.4
ZachWhite	1439	95	6.6
Zavala	1439	106	13.6
Zavala 2	1439	227	15.8
Aoy 2	1364	116	8.5
Aoy	1120	346	30.9
Hawkins	1394	343	24.6
UACJ_PAC01	1418	216	15.2
UACJ_PAC02	1437	98	6.8
UACJ_PAC03	1437	464	32.3
UACJ_PAC04	1429	208	14.6
UACJ_PAC05	1429	78	5.5
UACJ_PAC06	1429	89	6.2
UACJ_PAC08	1438	75	5.2
UACJ_PAC09	1430	110	7.7
UACJ_PAC10	1439	212	14.7
UACJ_PAC11	1433	73	5.1
UACJ_PAC12	1439	75	5.2
UACJ_PAC13	1439	61	4.2
UACJ_PAC14	1365	798	58.5
UACJ_PAC15	1439	1072	74.5
UACJ_PAC16	1437	115	8.0
UACJ_PAC17	1437	67	4.7
UACJ_PAC18	1437	55	3.8
UACJ_PAC19	1162	74	6.4
UACJ_PAC20	1162	72	6.2
UACJ_PAC21	550	36	6.5
UACJ_PAC22	549	34	6.2
UACJ_PAC23	1044	68	6.5
UACJ_PAC24	1044	72	6.9
UACJ_PAC25	883	55	6.2
UACJ_PAC26	883	56	6.3
UACJ_PAC27	930	332	35.7
UACJ_PAC28	829	37	4.5

3.6. COLLOCATED SENSORS PRE-DEPLOYMENT

As the US EPA and other studies recommended, the sensors must be calibrated before deployment at their sites. This pre-deployment period required 48 sensors to be deployed at a federal monitoring station. Instead, the sensors were collocated next to TCEQ's CAMS 12, near The University of Texas at El Paso.

The sensors remained at CAMS 12 for 14 days from December 2020 through January 2021. The sensor's data was stored in PurpleAir's cloud-based server and retrieved for the given time. The data set was then cleaned for outliers and processed to be used for the multiple variable regression model.

3.7. REGRESSION MODELS FOR SENSOR CORRECTION FACTOR

As stated previously, low-cost sensors lack the accuracy of regulatory monitors; as such, different regression techniques were utilized to bring the sensors more in line with FRM/FEM monitors. A multiple regression model analyzes the relationship between two or more variables to predict a value for the dependent variables. This regression aims to find the pollutant's dependency on more than one independent variable.

A multiple regression analysis was developed to correct the slope and intercept values of the low-cost sensors. The calibration involved the low-cost sensors and the reference stations, where the low-cost sensors were the independent variable (x), and the reference station was the dependent variable (y). The multiple regression is shown in Equation 8.

$$Ref = \beta_0 + \beta_1(Sensor) + \beta_2(\mathrm{RH}) + \beta_3(Temp) + \mathcal{E} \quad (8)$$

3.8. LAND-USE REGRESSION MODELING

Due to the spatial variability of air pollution in the basin, a land use regression model was utilized to explain and predict spatial contrasts in the PdN. LUR is a regression model used for analyzing pollution in dense areas; it has engineering applications and is used in many epidemiological studies to estimate concentrations at different locations [116].

LUR relies on a densely populated monitoring network; in this case, the network was based on the 48 deployed sensors in the PdN and a few regulatory monitors in El Paso. In addition, each site has specific "predictor values" gathered from ArcGIS and OpenStreetMap.

3.8.1 OPENSTREETMAP

This thesis uses data provided by OpenStreetMap. “OpenStreetMap contributors and available from https://www.openstreetmap.org copyright map data.” OpenStreetMap is open source, providing users with map data. OpenStreetMap is primarily built by the community; it is a community-driven project to create a comprehensive GIS map.

CHAPTER 4: STATISTICAL METHODS

4.1 LINEAR REGRESSION ANALYSIS

As mentioned in Chapter 2.3.3, calibration techniques are used to create calibration models to better fit the low-cost sensors with regulatory monitors. Simple linear regression models the relationship between two variables by fitting a linear equation over the data sets [117]. Two variables will be analyzed to determine the correlation between the two variables [118], and a linear relationship is expected between the FRM/FEM and low-cost sensors.

$$y = \alpha + \beta x + \epsilon \quad (9)$$

Equation 9 shows a simple linear regression where x is the independent variable and y is the dependent variable, α & β are the model parameters, and ε is the unpredictable random disturbance term or the error in predicting the value of y; it is important to note that this value is not displayed in most regression equations; instead, it will be similar to Equation 9 [117]. Equation 11 shows the general equation of a straight line, where m is the gradient of the line and c is the y-intercept, x is the independent variable, and y is the dependent variable [119]

The regression equation's functionality is assessed through the coefficient of determination (R^2), standard error of the estimated value of β, and an F test. The R^2 was primarily used in this thesis to determine how well the model fits the data. Most commonly, the R^2 will vary from 0 through 1, where at 0, none of the variances between variables can be explained, and 1, where all variations in y can be explained by independent variables [117].

4.2 MULTIPLE REGRESSION MODEL

Like the simple linear regression model, the multiple regression model establishes the relationship between two or more variables where there is more than one independent variable in

this regression. The objective of the multiple regression model is to utilize the independent variables to predict the value of a singular dependent variable [120].

$$y = \beta_0 + \beta_1 x_{i_1} + \beta_2 x_{i_2} + \cdots + \beta_p x_{i_p} + \epsilon \quad (10)$$

In Equation 10, Y is denoted as the dependent variable, and $X_1,\ldots, X_n$ is the dependent variable. The importance of each variable is pivotal to ensuring the maximal prediction of the dependent variable [120]. Equation 10 also shows the formula of multiple linear regressions, where y is the dependent variable, x_i is the explanatory variable, β_0 is the y-intercept, β_p is the slope coefficient, and ϵ is the model's error or residual.

CHAPTER 5: LOW-COST SENSOR CALIBRATION AND QUALITY CONTROL

5.1. SIDE-BY-SIDE COMPARISON LOW-COST SENSOR AND TCEQ CAMS STATION

The low-cost sensors were collocated next to a federal monitoring station (CAMS-12) for a 2-week calibration process. Calibration was necessary to develop a correction equation applied to the sensors once deployed across the PdN. This collocation period was conducted at a UTEP facility less than 10 feet away from CAMS 12's samplers for 48 low-cost sensors, as seen in Figure 6.

Figure 6: PA-II-SD deployed next to TCEQ CAMS 12 Station

The data was then collected for the 48 low-cost sensors and processed according to the specifications discussed in subchapter 3.5. Data outside the specific parameters were flagged and not processed, as it was removed from the raw two-minute data set. The "cleaned" two-minute data were then averaged into hourly intervals for the following parameters: $PM_{2.5}$, temperature, and relative humidity.

In addition, temperature and relative humidity were found to affect $PM_{2.5}$ significantly; this is especially true for relative humidity, which had a more significant effect on the optical capability of the sensor [121]–[123]. Due to this, $PM_{2.5}$, temperature, and relative humidity were used as predictor variables (x-variables) to better predict or fit the data with the reference station. A linear regression model was then used to produce the coefficients for each parameter. It is important to note that the linear regression model showed an overall summary statistic for the regression model; however, this output does not provide the beta coefficients. Therefore, the coefficients in the output need to be standardized utilizing the standard deviations of each of the variables.

The standardized or beta coefficients were utilized to create a correction factor for the data sets. However, it is important to note that each sensor had its individual correction factor, as each standardized coefficient varied by the sensor. The correction factor was applied to the sensor's hourly averaged data and was then compared to the FRM/FEM site to estimate the model's efficacy.

All sensors showed a high affinity with CAMS-12 before the correction equation. However, when the correction was applied to all 48 sensors, the sensors showed an increase in correlation when compared to CAMS-12, with most of the sensors showing an R^2 of 0.90-0.92, with the lowest R^2 being for the sensors: Aoy, UACJ-PAC22, and C12 with an R^2 between 0.88-0.89. Table 9 provides the R^2 for each of the 48 sensors used throughout the study. The beta coefficients were used continuously throughout the study to correct each sensor’s data.

Table 9: Correlation between Low-Vost Sensors and CAMS12

Site	R^2 corrected		Site	R^2 corrected
Hawkins	0.92		UACJ-PAC01	0.90
Zavala	0.92		UACJ-PAC22	0.89
Mesita	0.92		UACJ-PAC21	0.92
Aoy 2	0.92		UACJ-PAC20	0.92
CAMS12	0.89		UACJ-PAC19	0.90
CAMS12	0.90		UACJ-PAC23	0.92
CAMS 7	0.91		UACJ-PAC24	0.92
Whitaker	0.92		UACJ-PAC17	0.91
Douglass	0.92		UACJ-PAC18	0.91
Aoy	0.88		UACJ-PAC25	0.92
Park	0.92		UACJ-PAC26	0.92
Coldwell	0.90		SPARE	0.92
Cielo Vista	0.92		UACJ-PAC15	0.92
Zach White	0.91		UACJ-PAC05	0.92
Western Hills	0.92		UACJ-PAC06	0.92
UACJ-PAC07	0.91		UACJ-PAC08	0.92
UACJ-PAC11	0.90		UACJ-PAC28	0.91
UACJ-PAC27	0.91		UACJ-PAC02	0.92
UACJ-PAC12	0.84		UACJ-PAC03	0.92
UACJ-PAC13	0.90		UACJ-PAC09	0.90
UACJ-PAC16	0.91		UACJ-PAC10	0.91
Park 2	0.94		SPARE	0.91
Zavala 2	0.91		UACJ-PAC14	0.92
Bonham	0.92		UACJ-PAC04	0.91

5.2 INTERCHANNEL COMPARISON FOR LOW-COST SENSORS

The PA-II-SD low-cost sensor is equipped with dual Plantower PMS5003 light scattering sensors; Purple Air will refer to each sensor as channel A or channel B. Both channels collect and report data every two minutes. As such, the data generated per sensor will have two data sets for $PM_{2.5}$ and a particular data set for RH and temperature. Previous literature has shown that sensors show a high correlation between each inner sensor or inter-channel [80], [124].

The confidence interval (CI) between the channels, as shown on the PurpleAir website, can be used as a preliminary snapshot of the sensor's conditions. However, this study looked at the inter-channel correlation for each of the 48 sensors. The lower correlation between channel A and channel B was used to identify sensors that were malfunctioning or that were beginning to malfunction. While the inner mechanics of each sensor could malfunction, it is essential to note that real-world conditions could also cause degradation within the sensor. For example, sensors

are exposed to myriad shapes, in which the sensor channels can be affected by debris or insects nesting within the sensor.

Channel-to-channel comparisons were plotted to find the congruency between their inner channels. As seen in Table 10, sensors located in El Paso had high linearity internal within their sensors, with most sensors having an R^2 of 0.98-0.99, except for the sensor located in the Whittaker site having an R^2 of 0.87. As can be seen, the sensors undergo a slight variation in $R^{2,}$ but this was a common factor, as most sensors would become downgraded during meteorological events or due to insects crawling within the sensor. Similarly, sensors located in Cd. Juarez had high linearity between each of the sensor's channels; as can be seen, most of the sensors had a high R^2 of 0.99 except for the sensor located at the UACJ-PAC14 and UACJ-PAC27 site, which had an R^2 of 0.86 and 0.87.

Table 10: Inter-Channel R2 for Low-Cost Sensor

Sensor	**R^2**	**Sensor**	**R^2**
UTEP 1	0.99	UACJ-PAC01	0.99
UTEP 2	0.96	UACJ-PAC02	0.99
UTEP 3	0.88	UACJ-PAC03	0.93
Bonham ES	0.99	UACJ-PAC04	0.98
Park 2	0.99	UACJ-PAC05	0.99
Park	0.95	UACJ-PAC06	0.98
Whitetaker	0.87	UACJ-PAC21	0.97
WesternHills	0.97	UACJ-PAC10	0.98
Mesita	0.99	UACJ-PAC09	0.99
Douglass	0.98	UACJ-PAC08	0.99
Cielo Vista	0.96	UACJ-PAC11	0.99
Aoy	0.91	UACJ-PAC12	0.99
Aoy 2	0.99	UACJ-PAC13	0.99
ZachWhite	0.98	UACJ-PAC14	0.86
Zavala 2	0.99	UACJ-PAC15	0.92
Zavala	0.99	UACJ-PAC16	0.99
		UACJ-PAC17	0.99
		UACJ-PAC18	0.99
		UACJ-PAC20	0.99
		UACJ-PAC19	0.99
		UACJ-PAC22	0.99
		UACJ-PAC23	0.99
		UACJ-PAC24	0.99
		UACJ-PAC25	0.99
		UACJ-PAC26	0.99
		UACJ-PAC27	0.87
		UACJ-PAC28	0.99
		UACJ-PAC07	0.99

It is important to note that the degradation of the sensor could also be caused by the sensor's operational time, meaning that the longer the sensor is in use, the higher the probability of the sensor malfunctioning, as shown in recent literature [125]–[127]. Although however, this is not to say that a newer sensor will be more precise and have higher accuracy; as seen in the table above, the sensors deployed in El Paso still had a high congruity between each other even though they were not recently acquired units.

5.3 SENSOR TO SENSOR COMPARISON

As mentioned previously, the inter-sensor correlation is an essential factor in determining the efficacy of the instrument. However, it is also vital to ensure that the sensor's channels are operating optimally; for this, the sensor was compared with each other to ensure that the sensor was working. A high correlation between sensor one and sensor two can be used to determine if a unit is becoming degraded or has ceased to work.

This study used 12 monitoring sites containing duplicated sensors, representing roughly 38% of the entire monitoring network in the Paso del Norte region. These sensors were used as another form of quality assurance. To avoid bias, the sites with duplicated sensors were selected randomly, except for the sensors located within the calibration site. Table 11 shows the 12 sites and how they correlated with each other. The sensors located in El Paso had a high correlation with each other ($R^2 > 0.94$), and the sensors located in Cd. Juarez had a high correlation as well ($R^2 > 0.96$). This high correlation between them showed that the instruments were working well. However, it is essential to note that the instruments correlated well with other PA-II-SD.

Table 11: Low-Cost Sensors Duplicated Sensors Inter-Channel R^2

Name on PurpleAir Website	**R^2**
Zavala 2	0.9850
Zavala	
Aoy 2	0.9555
Aoy	
Park 2	0.9779
Park	
UTEP 3	0.9849
UTEP 1	
UTEP 2	0.9961
UTEP 1	
UTEP 2	0.9414
UTEP 3	
UACJ-PAC22	0.9928
UACJ-PAC21	
UACJ-PAC20	0.9676
UACJ-PAC19	
UACJ-PAC23	0.9777
UACJ-PAC24	
UACJ-PAC26	0.9878
UACJ-PAC25	
UACJ-PAC09	0.9798
UACJ-PAC10	
UACJ-PAC02	0.9752
UACJ-PAC03	
UACJ-PAC17	0.9949
UACJ-PAC18	
UACJ-PAC05	0.9699
UACJ-PAC06	

CHAPTER 6: LAND USE REGRESSION MODELING

6.1. LAND USE REGRESION MODELING CONSIDERATIONS

Previous linear regression models have been primarily based on ground-level federal monitoring stations to predict and assess pollution concentrations [128], [129]. However, the emerging technology of low-cost sensors has made it more feasible to create LUR models with higher levels of detail due to the size of some networking communities. As well as community mapping has made it easier to obtain detailed information on cities with little geographical and community data. The 48 sensors were used to develop a LUR model for $PM_{2.5}$ and PM_{10} concentrations in the PdN.

Data was gathered from a 500 m buffer zone developed at each sensor location to retrieve various physical features such as transportation, facilities, roads, developed land, undeveloped land, natural, railways, and shops. Roads comprised the overall street length, primary roads, secondary roads, and local roads within the 500 m buffer. Primary roads are considered highways within the buffer zone, secondary roads consist of ample avenues, and local roads are streets connected to a residence. The distance from the sensors to various locations was also utilized in the model; the variables included were distance to the nearest heliport, airport, railyard, and port of entry (POE). Census data was utilized to gather the number of homes and the population within that buffer zone. Land cover was also considered in the primary modeling stages and comprised the total % of developed and undeveloped land within the buffer zone. The data was gathered from various sources; OpenStreet Map was used for more community-specific data, and this data was gathered via surveys and from community knowledge. The rest of the data was gathered from government data banks, such as the National Oceanic and Atmospheric Administration, Topologically Integrated Geographic Encoding and Referencing System from the census bureau, and the US government.

6.2. VARIABLES SELECTED FOR LUR MODELING

A univariate analysis was employed before the LUR model was created to find the predictors with a high affinity with certain PM conditions. The predictors were used with different $PM_{2.5}$ and PM_{10} conditions during the study, such as the period average, the 24-hour max, and the one-hour max. Where a p-value less than 0.05 showed a statistical significance with the pollutant condition and the predictor, these were the predictors selected for the LUR model.

In Table 12, the LUR predictors were used in conjunction with $PM_{2.5}$ variables; the predictors used were street length, primary roads, secondary roads, local roads, distance to railyards, Texas Department of Transportation annual average daily traffic (TXDOT AADT), distance to POE, distance to a major arterial road (MAJART), total vehicle miles traveled (VMT), population, total housing units, % of developed/undeveloped land, distance to the refinery (REF), distance to the heliport, and the distance to the nearest airport. The p-value and R^2 are meaningful, with the p-value indicating if there is a significant relationship, and the R^2 measures the degree to which the data can be explained. As shown in Table 12, the p-values highlighted in red were statistically significant. In addition, distance to the nearest railyard, the total population, and total housing units had statistical significance for $PM_{2.5}$.

Table 12: Land Use Regression Variables Univariate Analysis against $PM_{2.5}$ Variables

Univariate Analysis						
$PM_{2.5}$	Period Average		24 Hour Max		1 Hour Max	
	p-Value	R^2	p-Value	R^2	p-Value	R^2
Street Length (mi)	0.43	0.09	0.22	0.18	0.28	0.16
Primary Roads (mi)	0.70	0.02	0.56	0.04	0.73	0.02
Secondary Roads(mi)	0.16	0.26	0.12	0.27	0.36	0.12
Local Roads (mi)	0.62	0.04	0.52	0.05	0.07	0.39
Distance to Railyard (mi)	**0.01**	0.82	**0.02**	0.50	0.10	0.33
TXDOT AADT (mi)	0.82	0.01	0.60	0.04	0.88	0.00
Distance To POE (mi)	0.14	0.28	0.66	0.03	0.29	0.16
Distance TO MAJART(mi)	0.30	0.15	0.08	0.34	0.21	0.21
TOT VMT (mi)	0.85	0.01	0.64	0.02	0.64	0.03
Population	**0.01**	0.60	**0.03**	0.48	0.08	0.37
Total Housing Units	**0.01**	0.60	0.06	0.38	**0.04**	0.48
% Developed Land	0.52	0.06	0.80	0.01	0.47	0.08
% Undeveloped	0.20	0.22	0.90	0.00	0.19	0.23
Distance to REF (mi)	0.69	0.02	0.64	0.02	0.16	0.27
Distance to Heliport (mi)	0.67	0.03	0.89	0.00	0.28	0.16
Distance to Airport (mi)	0.85	0.01	0.93	0.00	0.25	0.18

The PM_{10} variable also utilized the LUR predictors mentioned in the previous paragraph Table 13. There was a different variety in $PM_{2.5}$ and PM_{10} predictors, such as for local roads, distance to the nearest MAJART, and total VMT. The only shared predictor was the distance to the nearest railyard, with a 0.01 p-value for both $PM_{2.5}$ and PM_{10}.

Table 13: Land Use Regression Variables Univariate Analysis against PM_{10} Variables

Univariate Analysis						
PM_{10}	Period Average		24 Hour Max		1 Hour Max	
	p-Value	R^2	p-Value	R^2	p-Value	R^2
Street Length (mi)	0.25	0.18	0.34	0.11	0.37	0.17
Primary Roads (mi)	0.16	0.23	0.33	0.12	0.11	0.28
Secondary Roads (mi)	0.08	0.33	0.27	0.15	0.20	0.19
Local Roads (mi)	**0.04**	0.43	0.78	0.01	0.84	0.01
Railroads (mi)	0.63	0.02	0.18	0.22	0.52	0.05
Distance to Railyard (mi)	**0.01**	0.59	0.34	0.11	**0.04**	0.42
Distance To POE (mi)	0.15	0.24	0.51	0.05	0.28	0.15
Distance TO MAJART (mi)	**0.02**	0.52	0.74	0.01	0.40	0.09
TOT VMT (mi)	**0.01**	0.58	0.42	0.08	0.11	0.29
Population	0.38	0.09	0.46	0.07	0.88	0.00
Total Housing Units	0.39	0.09	0.78	0.02	0.81	0.01
% Developed Land	0.07	0.35	0.53	0.05	0.23	0.18
% Undeveloped	0.71	0.02	0.49	0.06	0.56	0.04
Distance to REF (mi)	0.15	0.24	0.98	0.00	0.39	0.09
Distance to Heliport (mi)	0.09	0.32	0.92	0.00	0.37	0.10
Distance to Airport (mi)	0.32	0.12	0.47	0.07	0.69	0.02

Following this univariate analysis, the following predictors were selected in the model based on their statistical significance and pollution condition: Street length, primary roads, distance to the nearest railyard, distance to the nearest POE, population, and houses were selected. Finally, a bivariate scatter plot was created with scatter plots below the diagonal, histograms on the diagonal, and a Pearson correlation above the diagonal, as seen in Figure 7, where there was a high correlation between distance to the POE and distance to the nearest railyard of 0.609 and a high correlation for houses and distance to the nearest POE of 0.744.

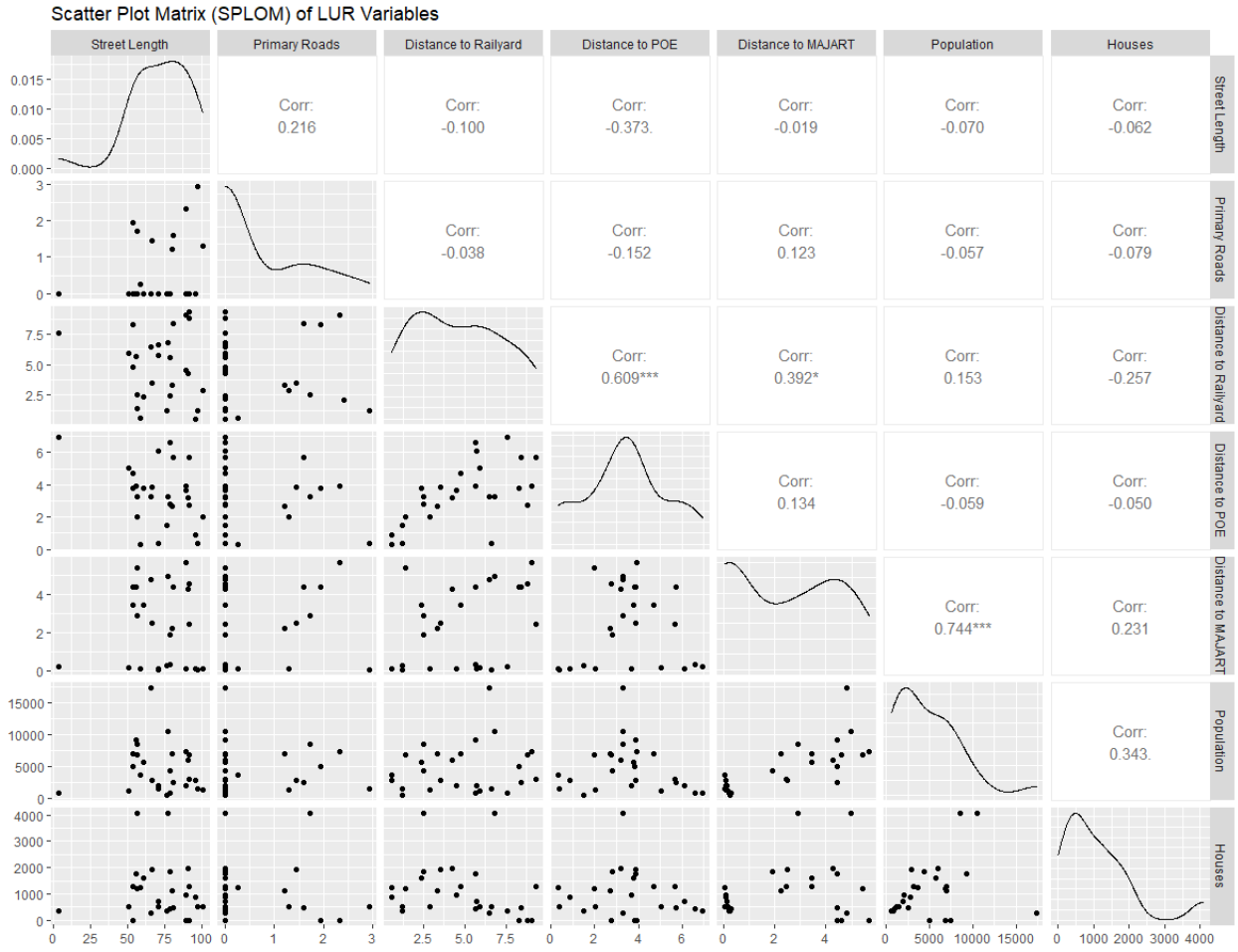

Figure 7: Scatter Plot Matrix of Selected LUR Variables

CHAPTER 7: RESULTS AND DISCUSSIONS

7.1. LOW-COST SENSOR PERFORMANCE IN THE EL PASO DEL NORTE REGION

The deployed sensors operated and recorded data that was to the specification of the PMS5003 sensor. As well as duplicated sensors, those being sites with two PA-II-SD sensors, reported data with high accuracy when compared with each other. Furthermore, these sensors had a high correlation with sites such as Aoy or Zavala having a high R^2 (>90%). As well as the sensor's inter-channel correlation had a high affinity with each other, this being channel A and channel B (R^2 <90%). These correlations showed that the sensors operated ideally for low-cost-to-low-cost performance.

A few sensors required further maintenance in the field, with two sensors in Cd. Juarez requiring extensive maintenance. These sensors were recording and reporting data that was out of the norm for the low-cost sensors, which degradation could have occurred with one of the PM sensors. As a result, the sensors were decommissioned and replaced; as their data continued to be out of the norm, even after being cleared of debris, it could be assumed that the sensor had a mechanical malfunction, degrading the PM sensors and rendering the data invalid.

7.1.1 $PM_{2.5}$ IN THE EL PASO DEL NORTE REGION

During the two-month deployment, the sensors provided real-time data to the community. Table 11 shows the summary statistics of the sensors and how the levels of concentration at the given sites. It was found that $PM_{2.5}$ fluctuated from 7.6-12.6 $\mu g/m^3$ in the PdN; this fluctuation is based on the 48 deployed sensors. The minimum $PM_{2.5}$ reported in the PdN was from one of the sensors located in Zach White in El Paso, with the minimum $PM_{2.5}$ recorded being 1.4 $\mu g/m^3$. A site in Mexico (UACJ-PAC11) had the highest maximum average in the PdN (81.9 $\mu g/m^3$). In-depth summary statistics for $PM_{2.5}$ can be seen in Table 14 for the other 32 sites. Information on PM_{10} summary statistics can be found in the Appendix under Table add number.

Table 14: Summary Statistics of $PM_{2.5}$ in El Paso and Cd. Juarez

$PM_{2.5}$ Summary Statistics				
Sensor	**Average**	**Standard Deviation**	**Minimum**	**Maximum**
Zavala	9.1	3.0	3.8	31.1
ZavalaEs	8.7	3.1	2.3	31.5
Hawkins	8.4	2.8	2.6	32.9
Bonham	9.4	3.1	2.3	33.7
Douglass	9.2	3.3	2.6	30.3
Coldwell	8.9	2.8	3.1	27.9
Aoy	10.1	3.8	3.7	36.2
AoyES	10.2	4.7	2.3	36.5
Mesita	8.7	2.7	3.4	28.6
Cielo Vista	8.7	2.7	2.8	31.1
Park2	8.8	2.6	2.7	26.9
ParkES	8.7	2.8	2.7	31.6
Whitaker	7.6	2.9	3.7	33.7
Western Hills	8.8	2.9	3.2	29.5
Zach White	9.3	3.5	1.4	29.0
UTEP 3	9.6	3.3	3.6	31.3
UTEP 2	8.8	2.9	2.9	27.7
UTEP 1	9.7	2.6	6.2	24.9
UACJ-PAC07	-	-	-	-
UACJ-PAC13	11.0	4.7	3.2	50.4
UACJ-PAC16	11.3	5.6	2.6	57.9
UACJ-PAC11	12.7	7.5	3.2	82.0
UACJ-PAC08	9.6	3.5	3.6	40.4
UACJ-PAC22	8.9	2.9	4.0	34.1
UACJ-PAC21	8.9	3.3	3.2	39.5
UACJ-PAC20	9.0	3.0	4.2	32.2
UACJ-PAC19	10.4	3.1	4.5	30.5
UACJ-PAC04	9.8	4.4	3.5	53.1
UACJ-PAC23	10.0	2.8	4.3	24.7
UACJ-PAC24	10.5	3.0	4.6	25.9
UACJ-PAC26	9.0	3.0	5.5	29.3
UACJ-PAC25	9.0	3.0	5.5	29.3
UACJ01	9.4	2.8	3.7	25.6
UACJ-PAC12	-	-	-	-
UACJ-PAC09	9.2	4.1	2.4	47.7
UACJ-PAC10	8.9	3.9	2.8	42.7
UACJ-PAC01	11.7	5.2	2.7	54.7
UACJ-PAC15**	12.3	7.1	3.4	43.7
UACJ-PAC28	9.6	3.1	5.3	25.7
UACJ-PAC14**	10.6	5.2	3.3	39.6
UACJ-PAC27	8.5	3.3	4.0	31.2
UACJ-PAC02	10.3	3.7	2.9	30.7
UACJ-PAC03	10.9	4.6	3.1	45.3
UACJ-PAC17	9.4	4.1	4.5	47.6
UACJ-PAC18	10.0	4.5	2.9	50.6
UACJ-PAC05	9.9	4.9	2.6	60.1
UACJ-PAC06	9.6	5.2	3.7	61.0

7.1.2 DIURNAL $PM_{2.5}$ VARIATION

Air pollutants vary diurnally, monthly, and seasonally depending on the climates and weather present [130], [131]. Local weather conditions, anthropogenic activities, and geographical variations, primarily influence emission variation. For example, $PM_{2.5}$ has different cycles throughout the day, with a peak occurring during the morning hours of 7:00 and 10:00 local solar time (LST) and having a peak early at night during 21:00 and 23:00 LST and a minimum being often seen between 15:00 and 17:00 LST [132].

$PM_{2.5}$ at the 32 sites followed a similar trend, with peaks in the afternoons or early evenings. $PM_{2.5}$ peaked between the hours of 4:00 through 9:00 Mountain Standard Time (MST), with low $PM_{2.5}$ concentrations occurring before high vehicular traffic flow at 6:00 MST. The diurnal patterns for the two sensors can be seen in Figure 8 for the sensors located in UTEP and UACJ; more sensor data can be seen in the appendix.

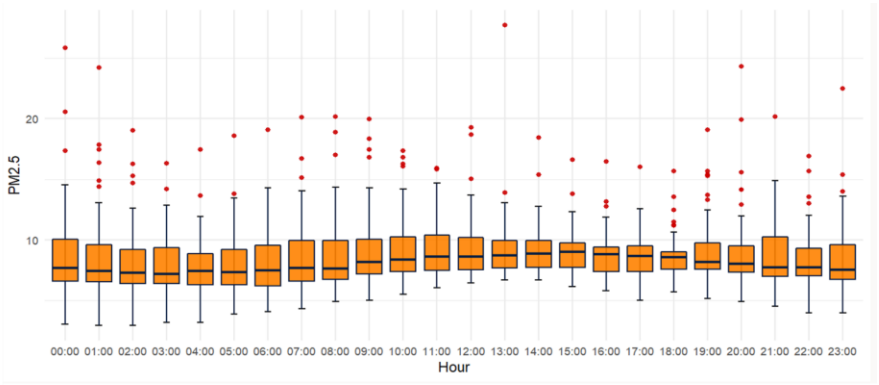

a) Hourly Boxplot for $PM_{2.5}$ during the study period: UTEP 1

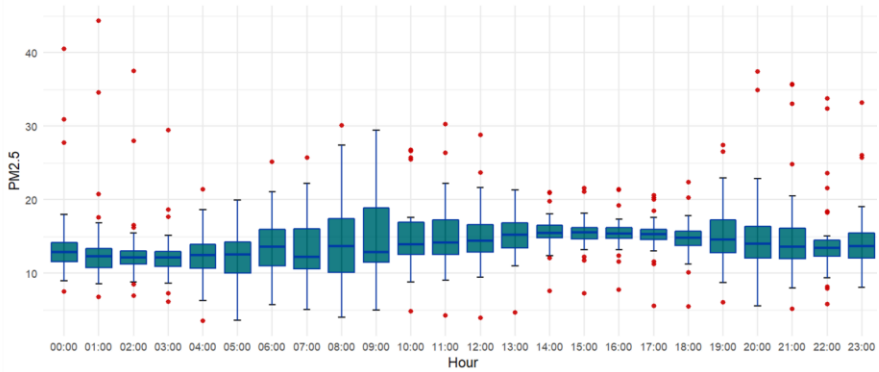

b) Hourly Boxplot for $PM_{2.5}$ during the study period: UACJ01

Figure 8: Daily PM2.5 Boxplots

The data gathered over the two months was also analyzed for weekly patterns, with some weekdays having higher concentrations than others. It was seen that the highest levels of concentration were during the weekends, on Saturday and Sunday, with 14 sites reporting the highest during Saturday and 13 sites reporting Sunday as the highest weekday. On the other hand, the lowest weekday during the two months was during Thursday for most of the sensors in the PdN. The weekday peaks can be seen below in Table 1Table 15.

Table 15: $PM_{2.5}$ Daily Highest Concentration throughout the week

Name on PurpleAir Website	Type of Site	Highest Weekday	Lowest Weekday
Zavala	Elementary School	Saturday	Thursday
ZavalaEs			
Hawkins	Elementary School	Saturday	Wednesday
Bonham	Elementary School	Saturday	Thursday
Douglass	Elementary School	Sunday	Thursday
Coldwell	Elementary School	-	-
Aoy	Elementary School	Sunday	Thursday
AoyES			
Mesita	Elementary School	Sunday	Thursday
Cielo Vista	Elementary School	Saturday	Thursday
Park2	Elementary School	Sunday	Thursday
ParkES			
Whitaker	Elementary School	Sunday	Wednesday
Western Hills	Elementary School	Sunday	Thursday
Zach White	Elementary School	Saturday	Thursday
UTEP 3	Calibration Site	Sunday	Thursday
UTEP 2			
UTEP 1			
UACJ-PAC07	Elementary School		
UACJ-PAC13	Elementary School	Saturday	Thursday
UACJ-PAC16	Elementary School	Sunday	Thursday
UACJ-PAC11	Elementary School	Sunday	Thursday
UACJ-PAC08	Industrial Sector	Saturday	Thursday
UACJ-PAC22	Industrial Sector	Sunday	Wednesday
UACJ-PAC21			
UACJ-PAC20	Industrial Sector	Saturday	Wednesday
UACJ-PAC19			
UACJ-PAC04	Industrial Sector	Sunday	Friday
UACJ-PAC23	Industrial Sector	Saturday	Thursday
UACJ-PAC24			
UACJ-PAC26	Industrial Sector	Saturday	Thursday
UACJ-PAC25			
UACJ01	Industrial Sector	Saturday	Wednesday
UACJ-PAC12	Elementary School	Sunday	Thursday
UACJ-PAC09	Industrial Sector	Sunday	Thursday
UACJ-PAC10			
UACJ-PAC01	Industrial Sector	Saturday	Thursday
UACJ-PAC15	Industrial Sector	NA	NA
UACJ-PAC28			
UACJ-PAC14	Industrial Sector	NA	NA
UACJ-PAC27			
UACJ-PAC02	Industrial Sector	Saturday	Thursday
UACJ-PAC03			
UACJ-PAC17	Industrial Sector	Sunday	Thursday
UACJ-PAC18			
UACJ-PAC05	Industrial Sector	Saturday	Thursday
UACJ-PAC06			

7.1.3 METEOROLOGICAL DATA IN THE EL PASO DEL NORTE REGION

The temperature statistics can be seen in Table 16. The sensors' averages range from 66.9 ºF to 73.7 ºF, and maximums are reported of 116.5 ºF and a minimum of 33.5 ºF. It is important to note that these temperatures were never meant to reflect the environmental readings, as many variables can affect a sensor's temperature readings. For example, the PA-II-SD sensor could have higher readings than the environment due to heat being generated internally from the sensor’s component and the level of sun exposure.

Table 16.:Temperature Summary Statistics in El Paso and Cd. Juarez

Temperature				
Name on PurpleAir Website	**Average**	**Standard deviation**	**Minimum**	**Maximum**
Zavala 2	68.5	12.4	39.3	99.6
ZavalaEs	69.8	13.8	39.8	111.2
Hawkins	70.9	13.0	40.3	102.2
Bonham	68.7	13.2	38.3	103.8
Douglass	70.5	11.7	42.9	98.7
Coldwell	69.0	13.4	41.6	101.2
Aoy 2	73.0	13.0	42.0	104.9
AoyES	67.0	12.0	39.7	98.1
Mesita	71.6	13.3	41.3	103.7
Cielo Vista	70.5	14.2	37.0	105.0
Park 2	68.9	11.6	38.0	92.6
ParkES	68.5	12.1	38.7	97.5
Whitaker	70.2	12.2	42.9	99.7
Western Hills	69.4	13.9	36.3	104.7
Zach White	69.6	14.0	39.2	108.2
UTEP 3	67.8	12.7	38.7	100.4
UTEP 2	68.2	12.4	39.5	100.2
UTEP 1	72.0	11.9	47.0	101.6
UACJ-PAC07	-	-	-	-
UACJ-PAC13	69.9	14.5	35.6	110.6
UACJ-PAC16	68.2	13.1	35.5	99.4
UACJ-PAC11	71.4	13.4	40.2	105.0
UACJ-PAC08	69.3	14.1	36.3	104.4
UACJ-PAC22	68.1	12.2	40.6	97.1
UACJ-PAC21	66.9	11.7	40.2	95.0
UACJ-PAC20	70.0	12.6	39.7	98.7
UACJ-PAC19	69.1	12.5	39.3	98.3
UACJ-PAC04	68.8	13.4	36.3	101.8
UACJ-PAC23	70.8	12.4	42.6	98.9
UACJ-PAC24	69.7	12.6	40.5	98.5
UACJ-PAC26	73.7	13.6	44.9	104.5
UACJ-PAC25	73.7	13.6	44.9	104.5
UACJ01	69.8	14.7	38.7	116.5
UACJ-PAC12	69.6	12.7	38.2	99.9
UACJ-PAC09	69.0	13.1	38.3	102.1
UACJ-PAC10	68.8	13.4	37.8	102.4
UACJ-PAC01	70.1	14.1	37.2	104.4
UACJ-PAC15**	69.2	13.2	36.6	101.1
UACJ-PAC28	73.1	12.0	48.0	99.5
UACJ-PAC14**	70.5	14.2	38.6	105.3
UACJ-PAC27	67.8	12.7	38.7	100.4
UACJ-PAC02	68.4	13.7	36.0	102.7
UACJ-PAC03	68.4	13.5	35.9	100.7
UACJ-PAC17	68.5	13.2	37.2	100.9
UACJ-PAC18	68.7	13.1	37.6	101.1
UACJ-PAC05	66.9	12.9	35.5	98.3
UACJ-PAC06	67.2	13.2	37.1	99.9

The PA-II-SD sensor also reports relative humidity; these values can be seen in Table 17, which are for the two-month study period. The average value recorded in the study is between 14.6 and 19.2%, having a minimum value of 0% and a maximum value of 70.6%. Most sensors had a minimum of <3 % and a maximum value of >50%.

Table 17: Summary Statistics Relative Humidity

Relative Humidity				
Sensors Name	**Average**	**Standard deviation**	**Minimum**	**Maximum**
Zavala	17.0	11.5	0.0	66.1
ZavalaEs	17.3	12.2	0.0	66.0
Hawkins	16.0	11.3	0.1	64.3
Bonham	16.2	12.2	0.0	65.9
Douglass	17.7	10.5	2.0	63.2
Coldwell	17.4	12.1	0.0	62.4
Aoy	15.7	11.0	0.0	59.4
AoyES	17.9	11.4	0.0	63.2
Mesita	16.3	11.0	0.1	57.6
Cielo Vista	16.8	11.8	0.0	63.5
Park2	18.3	12.7	1.0	69.1
ParkES	17.0	11.4	0.8	59.4
Whitaker	16.8	11.4	1.0	64.3
Western Hills	17.7	12.1	0.0	64.2
Zach White	19.2	11.2	1.2	58.1
UTEP 3	18.9	12.3	1.0	70.2
UTEP 2	18.1	12.1	1.0	69.0
UTEP 1	19.0	11.2	3.0	65.7
UACJ-PAC07	-	-	-	--
UACJ-PAC13	16.5	12.4	0.0	64.1
UACJ-PAC16	16.3	12.1	0.0	66.0
UACJ-PAC11	15.3	11.2	0.0	62.7
UACJ-PAC08	17.3	12.5	0.0	68.2
UACJ-PAC22	18.1	12.6	0.1	64.7
UACJ-PAC21	17.8	12.2	0.1	63.0
UACJ-PAC20	16.1	12.4	0.0	70.4
UACJ-PAC19	16.7	12.1	0.0	65.5
UACJ-PAC04	16.9	11.8	0.0	66.7
UACJ-PAC23	16.8	12.4	0.2	69.6
UACJ-PAC24	16.5	12.9	0.0	69.0
UACJ-PAC26	16.4	12.3	0.0	60.1
UACJ-PAC25	16.4	12.3	0.0	60.1
UACJ01	16.9	11.9	0.0	62.7
UACJ-PAC12	16.7	11.1	0.3	65.4
UACJ-PAC09	17.3	12.5	0.0	70.6
UACJ-PAC10	17.4	12.4	0.0	69.3
UACJ-PAC01	15.8	11.8	0.0	67.8
UACJ-PAC15**	17.0	11.8	0.0	63.6
UACJ-PAC28	14.6	11.6	0.0	62.9
UACJ-PAC14**	17.2	12.3	0.0	66.4
UACJ-PAC27	18.9	12.3	1.0	70.2
UACJ-PAC02	17.3	12.3	0.0	65.7
UACJ-PAC03	17.3	12.6	0.0	66.6
UACJ-PAC17	16.4	12.4	0.0	68.3
UACJ-PAC18	16.8	12.4	0.0	68.1
UACJ-PAC05	17.4	12.0	0.1	66.9
UACJ-PAC06	18.3	12.7	0.0	65.8

As mentioned previously, different meteorological conditions can have a dire effect on diurnal patterns for $PM_{2.5}$. Therefore, with wind direction and speed having a substantial effect on the dispersion of this pollutant, wind roses were created to explore further the met conditions in the El Paso and Cd. Juarez basins. Although this study showed that most of the wind arrived primarily from the west, this trend was seen through the two months. The wind roses are shown in Figure 9.

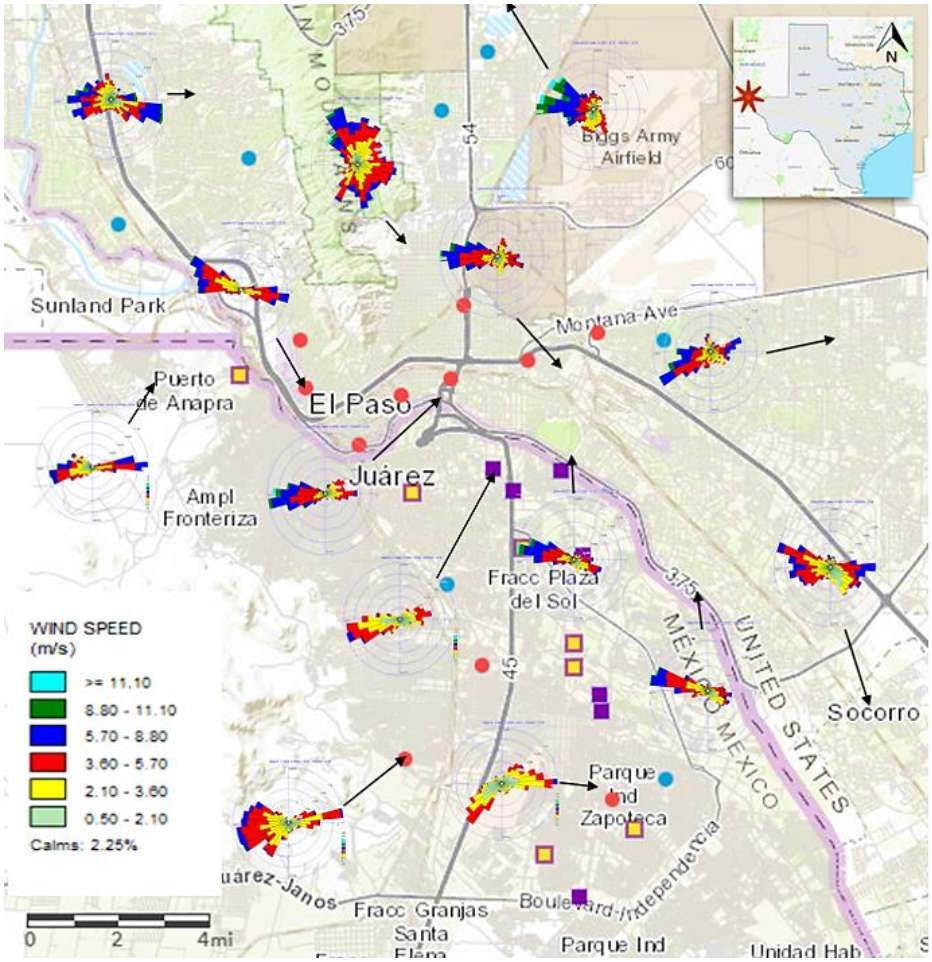

Figure 9: Wind Roses in the El Paso Del Norte

7.2. LAND USE REGRESSION MODELING OUTPUT

The generalized linear model that has not been optimized for the most significant variations can be seen in Table 18, where there are no variables showing a p-value less than 0.05. Showing that the model needs to be optimized further, to find the variables that could have a statistically significant value.

Table 18: Generalized Linear Model for $PM_{2.5}$ using selected LUR Variables

Y Variable	X Variable (in mi)	Estimate	Std. Error	t value	Pr(>|t|)	R^2	Adj. R^2
$PM_{2.5}$ Period Average	(Intercept)	5.30	0.36	14.93	0.00	0.31	0.06
	Sum Street Length (mi)	-0.01	0.02	-0.53	0.60		
	Primary Roads (mi)	0.29	0.43	0.67	0.51		
	Dis to Railyard (mi)	0.03	0.20	0.18	0.86		
	Dis to POE (mi)	-0.16	0.28	-0.57	0.57		
	Dis to MAJART (mi)	0.49	0.30	1.63	0.12		
	Population (one housing unit)	-0.0001	0.00016	-0.61	0.55		
	Houses	0.00046	0.00041	1.17	0.26		
$PM_{2.5}$ 24-Hour Max	(Intercept)	16.70	1.23	13.53	0.00	0.25	-0.02
	Sum Street Length (mi)	-0.07	0.07	-0.96	0.35		
	Primary Roads (mi)	0.61	1.51	0.40	0.69		
	Dis to Railyard (mi)	-0.41	0.69	-0.59	0.56		
	Dis to POE (mi)	-0.65	0.99	-0.66	0.52		
	Dis to MAJART (mi)	1.86	1.04	1.78	0.09		
	Population(1000 people)	-0.00033	0.00056	-0.57	0.58		
	Houses(one housing unit)	-0.00025	0.001436	-0.16	0.88		
$PM_{2.5}$ 1 Hour Max	(Intercept)	58.78	4.89	12.01	0.00	0.24	-0.04
	Sum Street Length (mi)	-0.09	0.27	-0.33	0.75		
	Primary Roads (mi)	-2.58	5.99	-0.43	0.67		
	Dis to Railyard (mi)	-3.48	2.75	-1.27	0.22		
	Dis to POE (mi)	1.10	3.92	0.28	0.78		
	Dis to MAJART(mi)	8.14	4.14	1.97	0.06		
	Population(1000 people)	-0.001	0.00022	-0.45	0.65		
	Houses(one housing unit)	-0.0046	0.0057	-0.82	0.42		

The generalized linear model in Table 19 has not yet been optimized for the variable with a stronger relationship with the PM_{10} variable. However, the population strongly correlated with varying PM_{10} variables. For example, the model shows that for every increase in the population the PM_{10} period average value would increase by 0.00020 $\mu g/m^3$.

Table 19: Generalized Linear Model for PM_{10} with LUR variables

Y Variable	X Variable	Estimate	Std. Error	t value	Pr(>|t|)	R^2	Adj. R^2
PM_{10}_P_ Avg	(Intercept)	5.30	0.21	25.30	0.00	0.54	0.36
	Sum Street Length (mi)	0.01	0.01	0.47	0.64		
	Primary Roads (mi)	0.50	0.25	2.03	0.06		
	Dis to Railyard (mi)	-0.19	0.12	-1.65	0.12		
	Dis to POE (mi)	0.09	0.16	0.55	0.59		
	Dis to MAJART (mi)	0.04	0.17	0.24	0.81		
	Population(1000 people)	0.00020	-0.000089	2.26	0.04		
	Houses(one housing unit)	-0.00074	0.00023	-3.22	0.00		
PM_{10}_24hr_Max	(Intercept)	16.47	0.48	34.65	0.00	0.20	-0.11
	Sum Street Length (mi)	-0.01	0.03	-0.16	0.87		
	Primary Roads (mi)	0.11	0.56	0.20	0.84		
	Dis to Railyard (mi)	0.40	0.26	1.52	0.15		
	Dis to POE (mi)	-0.03	0.37	-0.09	0.93		
	Dis to MAJART (mi)	-0.60	0.40	-1.51	0.15		
	Population(1000 people)	0.00022	0.00020	1.09	0.29		
	Houses(one housing unit)	0.00047	0.00052	0.91	0.38		
PM_{10}_1hr_ Max	(Intercept)	1.41	0.20	7.19	0.00	0.26	-0.03
	Sum Street Length (mi)	-0.01	0.01	-0.83	0.42		
	Primary Roads (mi)	-0.03	0.23	-0.13	0.90		
	Dis to Railyard (mi)	-0.03	0.11	-0.29	0.78		
	Dis to POE (mi)	-0.06	0.15	-0.39	0.70		
	Dis to MAJART (mi)	0.18	0.16	1.08	0.30		
	Population(1000 people)	-0.000084	-0.000083	-1.01	0.32		
	Houses(one housing unit)	0.00034	0.00021	1.61	0.13		

It was found that $PM_{2.5}$ had a statistically significant relationship with "Dis_to_MAJART," and "$PM_{2.5}$ period average." It was found that per each mile increase in the "Dis_to_MAJART," the $PM_{2.5}$ would increase by 0.43 $\mu g/m^3$, this can further be seen in **Error! Reference source not found.**. Furthermore, there is a borderline statistically significant value, between the "$PM_{2.5}$ 24-Hour Max" and the "Dis_to_MAJART," where per each mile increase to the "Dis_to_MAJART" there will be an increase in $PM_{2.5}$ of 1.16 $\mu g/m^3$.

Table 20: Generalized Linear Model II for PM2.5 using LUR variables that have a higher affinity with PM2.5

Yvar	Xvar	Estimate	Std. Error	t value	Pr(>|t|)	R^2	Adj. R^2
$PM_{2.5}$ Period Average	(Intercept)	5.29	0.33	16.16	0.00	0.22	0.19
	Dis_to_MAJART (mi)	0.43	0.16	2.67	0.01		
$PM_{2.5}$ 24-Hour Max	(Intercept)	16.60	1.14	14.50	0.00	0.15	0.11
	Dis_to_MAJART (mi)	1.16	0.56	2.06	0.05		
$PM_{2.5}$ 1 Hour Max	(Intercept)	58.25	4.50	12.95	0.00	0.14	0.11
	Dis_to_MAJART (mi)	4.45	2.30	1.93	0.06		

It was found that PM_{10} had a strong linear relationship with "Primary_Roads," "Dis_to_Railyard," "Population," and "Houses" for "PM_{10} period average," "PM_{10} 24 Hour Max," and "PM_{10} 1 Hour Max." For example, for each one-mile increase in primary roads, PM_{10} can increase by 0.51 $\mu g/m^3$ for PM_{10}, and an increase in population could cause an increase of 0.0002 $\mu g/m^3$ in PM_{10}, and an increase in houses could cause a 0.00071 $\mu g/m^3$ in PM_{10} for the Y variable, "PM_{10} period average. Finally, houses affected the hourly maximum PM_{10}, in which an increase in houses could lead to an increase of 0.00037 $\mu g/m^3$. This can further be seen in Table 21.

Table 21: Generalized Linear Model II for PM_{10} using selected LUR variables

Yvar	Xvar	Estimate	Std. Error	t value	Pr(>|t|)	R^2	Adj.R^2
PM_{10} Period Average	(Intercept)	5.31	0.19	27.65	0.00	0.52	0.43
	Primary_Roads(mi)	0.51	0.22	2.35	0.03		
	Dis_to_Railyard(mi)	-0.14	0.08	-1.82	0.08		
	Population(1000 people)	0.0002	-0.000057	3.54	0.00		
	Houses	0.00071	0.00021	-3.43	0.00		
PM_{10} 24-Hour Max	(Intercept)	16.47	0.43	38.29	0.00	0.16	0.05
	Dis_to_Railyard(mi)	0.31	0.18	1.72	0.10		
	Dis_to_MAJART(mi)	-0.53	0.35	-1.53	0.14		
	Population(1000 people)	0.00025	0.00017	1.47	0.16		
PM_{10} 1 Hour Max	(Intercept)	1.38	0.17	7.92	0.00	0.17	0.14
	Houses(one housing unit)	0.00037	0.00017	2.22	0.04		

CHAPTER 8: CONCLUSIONS AND RECOMMENDATIONS

8.1 LOW-COST SENSOR PERFORMANCE

Over the years, the use of low-cost air quality sensors has steadily increased, offering a cheap and easy solution for cheap air monitoring; as such, they have grown in popularity with the public and have garnered interest from institutions. Consequently, low-cost sensors have been widely applied to respond to high pollution areas and to ease the general public's worries. Nevertheless, there have been doubts regarding the accuracy and reliability of these units, especially when compared to the results reported from regulatory monitoring stations.

A $PM_{2.5}$ monitoring campaign was conducted for two months in March and April 2021, where the sensors were deployed across 32 sites, 12 in El Paso and 20 in Cd. Juarez, to establish a set of $PM_{2.5}$ data. The selection criteria for the sites were made according to the AADT, sites with low or high AADT. During the study period, the sensors worked to their specifications; this was shown in their inter-channel and inter-sensor correlations. However, it was found that the sensors were highly subjected to different environmental conditions that could degrade the internal components of the units. For example, an intense dust event during the study period affected six of the deployed sensors, where maintenance had to be conducted, and only three out of the six could be salvaged.

The low-cost sensors produced consistent data, showing a similar $PM_{2.5}$ mean trend among the sensors. As for the sensors located in El Paso, they showed that high AADT sites had slightly larger $PM_{2.5}$ concentrations (9.26±0.59) $\mu g/m^3$ than what was found in low AADT sites (8.63±0.54) $\mu g/m^3$. Cd. Juarez had two types of site locations: industrial and school zones. The school zones located in high AADT in Cd. Juarez showed values of 11.66±0.87 $\mu g/m^3$; unfortunately, the site located in the low AADT zone, was reporting values outside of the specifications of the manufacturer, and those data points were not included in this study. On the other hand, the industrial sites showed different levels; sites in high AADT zones were lower (9.48±0.61) $\mu g/m^3$ than what was seen in low AADT sites (10.06±1.07) $\mu g/m^3$, the cause of this

lower concentration was due to street work currently taking place in the city, which caused atypical vehicular flow. In general, it was found that $PM_{2.5}$ concentrations were lower in El Paso than in Cd. Juarez.

8.2. LAND-USE REGRESSION MODELING

The LUR modeling was conducted for two different pollutants, PM_{10} and $PM_{2.5,}$ using 10 different variables, with 3 variables for traffic conditions and 7 variables for the sum of street length, primary roads, distance to railyards, distance to the POE, distance to the MAJART, the population, and the number of homes. The predictor values were developed within a zone of influence of 500m in the radius for each of the 32 sites. It was found that the distance to the MAJART would increase the concentration of $PM_{2.5}$ by 0.43 $\mu g/m^3$ and 1.16 $\mu g/m^3$ for "$PM_{2.5}$ period average" and "$PM_{2.5}$ 24-hour max", respectively. In addition, for each mile increase in primary roads, PM_{10} was seen to increase by 0.51 $\mu g/m^3$, and an increase in PM_{10} by 0.14 $\mu g/m^3$ for the "PM_{10} period average" variable for each mile decrease to the nearest railyard.

8.3. FURTHER RESEARCH

The rapid demand for low-cost sensors has prompted manufacturers to develop and produce different low-cost sensors yearly. While technology advances, the sensor's accuracy, and precision, compared to a reference station, are still challenged while technology advances. Therefore, a correction factor must be developed and maintained throughout a project. Maintaining an extensive network of sensors can become cumbersome and create complications in sensor retrieval for re-calibration. As such, a general correction factor could be created from a singular sensor that remains at the reference station; this would allow the correction to be updated and adapted for different meteorological conditions.

The LUR model requires further research to identify different variables that can play a significant role in creating the model. In addition, as this model was done bi-nationally, it was not

easy to have the same level of detail in geographic and transportation data. Therefore, the model is limited to what is available for both countries. Also, the traffic variables are based on long-term measurements, which creates inconsistencies with the study periods.

REFERENCES

[1] J. Hooper and S. Marx, “A global doubling of dust emissions during the Anthropocene?,” *Glob. Planet. Change*, vol. 169, pp. 70–91, Oct. 2018, doi: 10.1016/J.GLOPLACHA.2018.07.003.

[2] S. P. Parajuli and C. S. Zender, “Projected changes in dust emissions and regional air quality due to the shrinking Salton Sea,” 2018, doi: 10.1016/j.aeolia.2018.05.004.

[3] W. Einfeld and H. W. Church, “Winter season air pollution in El Paso-Ciudad Juarez. A review of air pollution studies in an international airshed,” Mar. 1995, doi: 10.2172/45632.

[4] K. Klein Goldewijk, A. Beusen, G. Van Drecht, and M. De Vos, “The HYDE 3.1 spatially explicit database of human-induced global land-use change over the past 12,000 years,” *Glob. Ecol. Biogeogr.*, vol. 20, no. 1, pp. 73–86, Jan. 2011, doi: 10.1111/J.1466-8238.2010.00587.X.

[5] W.-W. Li, J. J. Bang, R. R. Chianelli, and M. J. Yacaman, “Characterization of Airborne Particulate Matter in the Paso del Norte Air Quality Basin: Morphology and Chemistry,” 2014, Accessed: Aug. 03, 2022. [Online]. Available: https://www.researchgate.net/publication/237763196.

[6] Texas Commission on Enviromental Quality, “The TCEQ’s Air Quality Programs in the Border Region - Texas Commission on Environmental Quality - www.tceq.texas.gov,” 2020. https://www.tceq.texas.gov/border/border-region-air-quality-programs (accessed Aug. 03, 2022).

[7] A. J. Cohen *et al.*, “Estimates and 25-year trends of the global burden of disease attributable to ambient air pollution: an analysis of data from the Global Burden of Diseases Study 2015,” *Lancet*, vol. 389, no. 10082, pp. 1907–1918, May 2017, doi: 10.1016/S0140-6736(17)30505-6.

[8] S. Pateraki *et al.*, “The traffic signature on the vertical PM profile: Environmental and health risks within an urban roadside environment,” *Sci. Total Environ.*, vol. 646, pp. 448–459, Jan. 2019, doi: 10.1016/J.SCITOTENV.2018.07.289.

[9] Y. Wang *et al.*, “Personal and household PM2.5 and black carbon exposure measures and respiratory symptoms in 8 low- and middle-income countries,” *Environ. Res.*, vol. 212, p. 113430, Sep. 2022, doi: 10.1016/J.ENVRES.2022.113430.

[10] X. Qiu *et al.*, “Inverse probability weighted distributed lag effects of short-term exposure to PM2.5 and ozone on CVD hospitalizations in New England Medicare participants - Exploring the causal effects,” *Environ. Res.*, vol. 182, p. 109095, Mar. 2020, doi: 10.1016/J.ENVRES.2019.109095.

[11] E. S. Coker, R. Buralli, A. F. Manrique, C. M. Kanai, A. K. Amegah, and N. Gouveia, “Association between PM2.5 and respiratory hospitalization in Rio Branco, Brazil: Demonstrating the potential of low-cost air quality sensor for epidemiologic research.,” *Environ. Res.*, vol. 214, p. 113738, Nov. 2022, doi: 10.1016/J.ENVRES.2022.113738.

[12] F. Liang, F. Liu, K. Huang, X. Yang, and D. Gu, “Reply: Long-Term Exposure to PM2.5 and CVD: The Role of Mir-486 and Genetic and Epigenetic Factors,” *J. Am. Coll. Cardiol.*, vol. 75, no. 22, pp. 2877–2878, Jun. 2020, doi: 10.1016/J.JACC.2020.04.026.

[13] M. Diao *et al.*, “Journal of the Air & Waste Management Association Methods, availability, and applications of PM 2.5 exposure estimates derived from ground measurements, satellite, and atmospheric models,” *Waste Manag. Assoc.*, vol. 69, pp.

1391–1414, 2019, doi: 10.1080/10962247.2019.1668498.
[14] G. Hoek *et al.*, “A review of land-use regression models to assess spatial variation of outdoor air pollution,” *Atmos. Environ.*, vol. 42, no. 33, pp. 7561–7578, Oct. 2008, doi: 10.1016/J.ATMOSENV.2008.05.057.
[15] M. He, Y. Zhong, Y. Chen, N. Zhong, and K. Lai, “Association of short-term exposure to air pollution with emergency visits for respiratory diseases in children,” *iScience*, p. 104879, Aug. 2022, doi: 10.1016/J.ISCI.2022.104879.
[16] M. D. Yazdi *et al.*, “The effect of long-term exposure to air pollution and seasonal temperature on hospital admissions with cardiovascular and respiratory disease in the United States: A difference-in-differences analysis,” *Sci. Total Environ.*, vol. 843, p. 156855, Oct. 2022, doi: 10.1016/J.SCITOTENV.2022.156855.
[17] L. Eades, “Air pollution at the U.S.- Mexico border: Strengthening the framework for bilateral cooperation,” *J. Public Int. Aff.*, vol. 2018, pp. 64–79, 2018, Accessed: Aug. 23, 2022. [Online]. Available: https://jpia.princeton.edu/sites/g/files/toruqf1661/files/resource-links/jpia_2018.pdf#page=64.
[18] J. E. Zora *et al.*, “Associations between urban air pollution and pediatric asthma control in El Paso, Texas,” *Sci. Total Environ.*, vol. 448, pp. 56–65, Mar. 2013, doi: 10.1016/J.SCITOTENV.2012.11.067.
[19] W. . Timmons, “TSHA | El Paso del Norte,” *TSHA*, 1995. https://www.tshaonline.org/handbook/entries/el-paso-del-norte (accessed Aug. 23, 2022).
[20] Office of the United StatesTrade Representative, “Mexico | United States Trade Representative,” 2019. https://ustr.gov/countries-regions/americas/mexico (accessed Aug. 23, 2022).
[21] P. J. E. Quintana *et al.*, “Traffic-related air pollution in the community of San Ysidro, CA, in relation to northbound vehicle wait times at the US–Mexico border Port of Entry,” *Atmos. Environ.*, vol. 88, pp. 353–361, May 2014, doi: 10.1016/J.ATMOSENV.2014.01.009.
[22] E. S. Park, D. W. Sullivan, D. H. Kang, Q. Ying, and C. H. Spiegelman, “Assessment of mobile source contributions in El Paso by PMF receptor modeling coupled with wind direction analysis,” *Sci. Total Environ.*, vol. 720, Jun. 2020, doi: 10.1016/J.SCITOTENV.2020.137527.
[23] U.S. Department of Transportation, “Border Crossing Entry Data | Tyler Data & Insights,” 2022. https://data.bts.gov/Research-and-Statistics/Border-Crossing-Entry-Data/keg4-3bc2/data (accessed Aug. 23, 2022).
[24] P. Agarwal, M. Sarkar, B. Chakraborty, and T. Banerjee, “Phytoremediation of Air Pollutants: Prospects and Challenges,” *Phytomanagement Polluted Sites Mark. Oppor. Sustain. Phytoremediation*, pp. 221–241, Dec. 2018, doi: 10.1016/B978-0-12-813912-7.00007-7.
[25] EPA, “Sources of Greenhouse Gas Emissions | US EPA,” 2022. https://www.epa.gov/ghgemissions/sources-greenhouse-gas-emissions (accessed Aug. 23, 2022).
[26] TCEQ, “Point Source Emissions Inventory - Texas Commission on Environmental Quality - www.tceq.texas.gov,” 2021. https://www.tceq.texas.gov/airquality/point-source-ei/psei.html (accessed Aug. 23, 2022).
[27] P. Phillips, “Factory Emissions,” Apr. 08, 2021.

https://storymaps.arcgis.com/stories/7221608f86ae406f802d294a51f690f3 (accessed Aug. 23, 2022).
[28] T. Favela, “El Paso ranks #4 in air pollution for mid-sized metros,” El paso, Jan. 29, 2020.
[29] H. Ritchie, “Climate change and flying: what share of global CO2 emissions come from aviation? - Our World in Data,” Oct. 22, 2020. https://ourworldindata.org/co2-emissions-from-aviation (accessed Oct. 20, 2022).
[30] S. Rodriguez, “EPIA Memo,” EL Paso , 2022. Accessed: Aug. 23, 2022. [Online]. Available: https://elpasointernationalairport.com/assets/documents/Airport/About/Operating-Reports/06-Jun-22-MD.pdf.
[31] USAPHC, “Particulate Matter (PM) Air Pollution Exposures During Military Deployments.”
[32] N. C. Crawford, “Pentagon Fuel Use, Climate Change, and the Costs of War,” 2019, Accessed: Oct. 20, 2022. [Online]. Available: https://watson.brown.edu/costsofwar/files/cow/imce/papers/2018/Crawford_Costs of War Es.
[33] J. A. Lee, M. C. Baddock, M. J. Mbuh, and T. E. Gill, “Geomorphic and land cover characteristics of aeolian dust sources in West Texas and eastern New Mexico, USA,” *Aeolian Res.*, vol. 3, no. 4, pp. 459–466, Jan. 2012, doi: 10.1016/J.AEOLIA.2011.08.001.
[34] N. P. Webb, B. L. Edwards, and C. Pierre, “Wind Erosion in Anthropogenic Environments,” *Treatise Geomorphol.*, pp. 301–319, 2022, doi: 10.1016/B978-0-12-818234-5.00031-6.
[35] J. E. Bullard *et al.*, “Preferential dust sources: A geomorphological classification designed for use in global dust-cycle models,” *J. Geophys. Res. Earth Surf.*, vol. 116, no. F4, p. 4034, Dec. 2011, doi: 10.1029/2011JF002061.
[36] K. Baca-López *et al.*, “Spatio-Temporal Representativeness of Air Quality Monitoring Stations in Mexico City: Implications for Public Health,” *Front. Public Heal.*, vol. 8, p. 849, Jan. 2021, doi: 10.3389/FPUBH.2020.536174/BIBTEX.
[37] Y. C. Lin, W. J. Chi, and Y. Q. Lin, “The improvement of spatial-temporal resolution of PM2.5 estimation based on micro-air quality sensors by using data fusion technique,” *Environ. Int.*, vol. 134, p. 105305, Jan. 2020, doi: 10.1016/J.ENVINT.2019.105305.
[38] W. J. Gauderman *et al.*, “Effect of exposure to traffic on lung development from 10 to 18 years of age: a cohort study,” *Lancet*, vol. 369, no. 9561, pp. 571–577, Feb. 2007, doi: 10.1016/S0140-6736(07)60037-3.
[39] World Health Organization, “WHO global air quality guidelines: particulate matter (PM2.5 and PM10), ozone, nitrogen dioxide, sulfur dioxide and carbon monoxide,” *World Heal. Organ.*, no. 9544, p. 1302, 2021.
[40] J. O. Anderson, J. G. Thundiyil, and A. Stolbach, “Clearing the Air: A Review of the Effects of Particulate Matter Air Pollution on Human Health,” *J. Med. Toxicol.*, vol. 8, no. 2, p. 166, Jun. 2012, doi: 10.1007/S13181-011-0203-1.
[41] H. R. Anderson, G. Favarato, and R. W. Atkinson, “Long-term exposure to air pollution and the incidence of asthma: meta-analysis of cohort studies,” *Air Qual. Atmos. Heal. 2011 61*, vol. 6, no. 1, pp. 47–56, Apr. 2011, doi: 10.1007/S11869-011-0144-5.
[42] W. Hinds, *Aerosol Technology Properties, Behavior, and Measurements of Airborne Particles*, 2nd ed. A Wiley-interscience, 1999.
[43] US EPA, “Particulate Matter (PM) Basics | US EPA,” Jul. 18, 2022.

https://www.epa.gov/pm-pollution/particulate-matter-pm-basics (accessed Sep. 01, 2022).
[44] Unites States Environmental Protection Agency, “Health and Environmental Effects of Particulate Matter (PM) | US EPA,” 2022. https://www.epa.gov/pm-pollution/health-and-environmental-effects-particulate-matter-pm (accessed Sep. 02, 2022).
[45] N. De Nevers, *Air Pollution Control Engineering*, 3rd ed. Waveland Press, 2017.
[46] Centers for Disease Control and Prevention, “Particle Pollution | Air | CDC,” 2022. https://www.cdc.gov/air/particulate_matter.html (accessed Sep. 02, 2022).
[47] W. J. Guan, X. Y. Zheng, K. F. Chung, and N. S. Zhong, “Impact of air pollution on the burden of chronic respiratory diseases in China: time for urgent action,” *Lancet*, vol. 388, no. 10054, pp. 1939–1951, Oct. 2016, doi: 10.1016/S0140-6736(16)31597-5.
[48] S. A. Rajper, S. Ullah, and Z. Li, “Exposure to air pollution and self-reported effects on Chinese students: A case study of 13 megacities,” *PLoS One*, vol. 13, no. 3, Mar. 2018, doi: 10.1371/JOURNAL.PONE.0194364.
[49] J. Shi *et al.*, “Cardiovascular benefits of wearing particulate-filtering respirators: A randomized crossover trial,” *Environ. Health Perspect.*, vol. 125, no. 2, pp. 175–180, Feb. 2017, doi: 10.1289/EHP73.
[50] H. Traboulsi, N. Guerrina, M. Iu, D. Maysinger, P. Ariya, and C. J. Baglole, “Inhaled pollutants: The molecular scene behind respiratory and systemic diseases associated with ultrafine particulate matter,” *Int. J. Mol. Sci.*, vol. 18, no. 2, Feb. 2017, doi: 10.3390/IJMS18020243.
[51] N. A. Assad, V. Kapoor, and A. Sood, “Biomass smoke exposure and chronic lung disease,” *Curr. Opin. Pulm. Med.*, vol. 22, no. 2, pp. 150–157, Mar. 2016, doi: 10.1097/MCP.0000000000000246.
[52] C. Carlsten, S. Salvi, G. W. K. Wong, and K. F. Chung, “Personal strategies to minimise effects of air pollution on respiratory health: advice for providers, patients and the public,” *Eur. Respir. J.*, vol. 55, no. 6, Jun. 2020, doi: 10.1183/13993003.02056-2019.
[53] United States Environmental Protection Agency, “NAAQS Table | US EPA,” 202AD. https://www.epa.gov/criteria-air-pollutants/naaqs-table (accessed Sep. 02, 2022).
[54] Environmental Protection Agency, “Frequently Asked Questions Frequently Asked Questions Near Roadway Air Pollution and Health: Frequently Asked Questions,” 2014.
[55] R. M. Lal, A. Ramaswami, and A. G. Russell, “Assessment of the Near-Road (monitoring) Network including comparison with nearby monitors within U.S. cities,” *Environ. Res. Lett.*, vol. 15, no. 11, p. 114026, Nov. 2020, doi: 10.1088/1748-9326/AB8156.
[56] G. Hagler *et al.*, “Evaluation of two collocated federal equivalent method PM2.5 instruments over a wide range of concentrations in Sarajevo, Bosnia and Herzegovina,” *Atmos. Pollut. Res.*, vol. 13, no. 4, p. 101374, Apr. 2022, doi: 10.1016/J.APR.2022.101374.
[57] Y. Kang, L. Aye, T. D. Ngo, and J. Zhou, “Performance evaluation of low-cost air quality sensors: A review,” *Sci. Total Environ.*, vol. 818, Apr. 2022, doi: 10.1016/J.SCITOTENV.2021.151769.
[58] T. C. Le *et al.*, “On the concentration differences between PM2.5 FEM monitors and FRM samplers,” *Atmos. Environ.*, vol. 222, p. 117138, Feb. 2020, doi: 10.1016/J.ATMOSENV.2019.117138.
[59] E. G. Snyder *et al.*, “The changing paradigm of air pollution monitoring,” *Environ. Sci. Technol.*, vol. 47, no. 20, pp. 11369–11377, Oct. 2013, doi:

10.1021/ES4022602/ASSET/IMAGES/LARGE/ES-2013-022602_0002.JPEG.
[60] M. R. Giordano *et al.*, "From low-cost sensors to high-quality data: A summary of challenges and best practices for effectively calibrating low-cost particulate matter mass sensors," *J. Aerosol Sci.*, vol. 158, p. 105833, Nov. 2021, doi: 10.1016/J.JAEROSCI.2021.105833.
[61] G. Vasquez, Y. Hernández, and Y. Coello, "Portable low-cost instrumentation for monitoring Rayleigh scattering from chemical sensors based on metallic nanoparticles," *Sci. Reports 2018 81*, vol. 8, no. 1, pp. 1–9, Oct. 2018, doi: 10.1038/s41598-018-33271-8.
[62] R. Acharya, "Interaction of waves with medium," *Satell. Signal Propagation, Impair. Mitig.*, pp. 57–86, Jan. 2017, doi: 10.1016/B978-0-12-809732-8.00003-X.
[63] K. M. Markowicz and M. T. Chiliński, "Evaluation of Two Low-Cost Optical Particle Counters for the Measurement of Ambient Aerosol Scattering Coefficient and Ångström Exponent," *Sensors 2020, Vol. 20, Page 2617*, vol. 20, no. 9, p. 2617, May 2020, doi: 10.3390/S20092617.
[64] J. Wallace and P. Hobbs, *Athmospheric Science*, 2nd ed. Elsevier, 2006.
[65] I. Vajs, D. Drajic, N. Gligoric, I. Radovanovic, and I. Popovic, "Developing Relative Humidity and Temperature Corrections for Low-Cost Sensors Using Machine Learning," *Sensors (Basel).*, vol. 21, no. 10, May 2021, doi: 10.3390/S21103338.
[66] A. Samad, D. R. O. Nuñez, G. C. S. Castillo, B. Laquai, and U. Vogt, "Effect of Relative Humidity and Air Temperature on the Results Obtained from Low-Cost Gas Sensors for Ambient Air Quality Measurements," *Sensors (Basel).*, vol. 20, no. 18, pp. 1–29, 2020, doi: 10.3390/S20185175.
[67] R. Jayaratne, X. Liu, P. Thai, M. Dunbabin, and L. Morawska, "The influence of humidity on the performance of a low-cost air particle mass sensor and the effect of atmospheric fog," *Atmos. Meas. Tech.*, vol. 11, no. 8, pp. 4883–4890, Aug. 2018, doi: 10.5194/AMT-11-4883-2018.
[68] I. Stavroulas *et al.*, "Field Evaluation of Low-Cost PM Sensors (Purple Air PA-II) Under Variable Urban Air Quality Conditions, in Greece," *Atmos. 2020, Vol. 11, Page 926*, vol. 11, no. 9, p. 926, Aug. 2020, doi: 10.3390/ATMOS11090926.
[69] M. Jovašević-Stojanović, A. Bartonova, D. Topalović, I. Lazović, B. Pokrić, and Z. Ristovski, "On the use of small and cheaper sensors and devices for indicative citizen-based monitoring of respirable particulate matter," *Environ. Pollut.*, vol. 206, pp. 696–704, Nov. 2015, doi: 10.1016/J.ENVPOL.2015.08.035.
[70] A. C. Rai *et al.*, "End-user perspective of low-cost sensors for outdoor air pollution monitoring," *Sci. Total Environ.*, vol. 607–608, pp. 691–705, Dec. 2017, doi: 10.1016/J.SCITOTENV.2017.06.266.
[71] Y. Wang, J. Li, H. Jing, Q. Zhang, J. Jiang, and P. Biswas, "Laboratory Evaluation and Calibration of Three Low-Cost Particle Sensors for Particulate Matter Measurement," *http://dx.doi.org/10.1080/02786826.2015.1100710*, vol. 49, no. 11, pp. 1063–1077, Nov. 2015, doi: 10.1080/02786826.2015.1100710.
[72] D. Wu *et al.*, "Influence of particle properties and environmental factors on the performance of typical particle monitors and low-cost particle sensors in the market of China," *Atmos. Environ.*, vol. 268, p. 118825, Jan. 2022, doi: 10.1016/J.ATMOSENV.2021.118825.
[73] M. Badura, P. Batog, A. Drzeniecka-Osiadacz, and P. Modzel, "Regression methods in the calibration of low-cost sensors for ambient particulate matter measurements," *SN Appl.*

Sci., vol. 1, no. 6, pp. 1–11, Jun. 2019, doi: 10.1007/S42452-019-0630-1/TABLES/5.
[74] Y. Wang, J. Li, H. Jing, Q. Zhang, J. Jiang, and P. Biswas, "Laboratory Evaluation and Calibration of Three Low-Cost Particle Sensors for Particulate Matter Measurement," *Aerosol Sci. Technol.*, vol. 49, no. 11, pp. 1063–1077, Nov. 2015, doi: 10.1080/02786826.2015.1100710.
[75] M. L. Zamora, J. Rice, and K. Koehler, "One year evaluation of three low-cost PM2.5 monitors," *Atmos. Environ.*, vol. 235, Aug. 2020, doi: 10.1016/j.atmosenv.2020.117615.
[76] J. Tryner *et al.*, "Laboratory evaluation of low-cost PurpleAir PM monitors and in-field correction using co-located portable filter samplers," *Atmos. Environ.*, vol. 220, p. 117067, Jan. 2020, doi: 10.1016/J.ATMOSENV.2019.117067.
[77] B. I. Magi, C. Cupini, J. Francis, M. Green, and C. Hauser, "Aerosol Science and Technology Evaluation of PM2.5 measured in an urban setting using a low-cost optical particle counter and a Federal Equivalent Method Beta Attenuation Monitor Evaluation of PM2.5 measured in an urban setting using a low-cost optical pa," 2020, doi: 10.1080/02786826.2019.1619915.
[78] C. Malings *et al.*, "Aerosol Science and Technology Fine particle mass monitoring with low-cost sensors: Corrections and long-term performance evaluation Fine particle mass monitoring with low-cost sensors: Corrections and long-term performance evaluation," 2019, doi: 10.1080/02786826.2019.1623863.
[79] K. Ko, S. Cho, and R. R. Rao, "Performance evaluation of low-cost purpleair sensors in ambient air," *Proc. - 2020 IEEE 7th Int. Conf. Data Sci. Adv. Anal. DSAA 2020*, pp. 563–568, Oct. 2020, doi: 10.1109/DSAA49011.2020.00071.
[80] L. Wallace, T. Zhao, and N. E. Klepeis, "Calibration of PurpleAir PA-I and PA-II Monitors Using Daily Mean PM2.5 Concentrations Measured in California, Washington, and Oregon from 2017 to 2021," *Sensors 2022, Vol. 22, Page 4741*, vol. 22, no. 13, p. 4741, Jun. 2022, doi: 10.3390/S22134741.
[81] J. Liu *et al.*, "Cokriging with a low-cost sensor network to estimate spatial variation of brake and tire-wear metals and oxidative stress potential in Southern California," *Environ. Int.*, vol. 168, p. 107481, Oct. 2022, doi: 10.1016/J.ENVINT.2022.107481.
[82] A. L. de Jesus *et al.*, "Ultrafine particles and PM2.5 in the air of cities around the world: Are they representative of each other?," *Environ. Int.*, vol. 129, pp. 118–135, Aug. 2019, doi: 10.1016/j.envint.2019.05.021.
[83] M. Tagle *et al.*, "Field performance of a low-cost sensor in the monitoring of particulate matter in Santiago, Chile," *Environ. Monit. Assess.*, vol. 192, no. 3, pp. 1–18, Mar. 2020, doi: 10.1007/S10661-020-8118-4/TABLES/3.
[84] Weatherbase, "Los Angeles, California Climate Classification (Weatherbase)," 2020. http://www.weatherbase.com/weather/weather-summary.php3?s=159227&cityname=Los+Angeles,+California,+United+States+of+America (accessed Sep. 12, 2022).
[85] J. Bi *et al.*, "Publicly available low-cost sensor measurements for PM2.5 exposure modeling: Guidance for monitor deployment and data selection," *Environ. Int.*, vol. 158, p. 106897, Jan. 2022, doi: 10.1016/J.ENVINT.2021.106897.
[86] D. M. Broday *et al.*, "Wireless distributed environmental sensor networks for air pollution measurement-the promise and the current reality," *Sensors (Switzerland)*, vol. 17, no. 10, Oct. 2017, doi: 10.3390/S17102263.
[87] G. N. Carvlin *et al.*, "Development and field validation of a community-engaged

particulate matter air quality monitoring network in Imperial, California, USA," *J. Air Waste Manag. Assoc.*, vol. 67, no. 12, pp. 1342–1352, Dec. 2017, doi: 10.1080/10962247.2017.1369471.

[88] E. M. Considine, C. E. Reid, M. R. Ogletree, and T. Dye, "Improving accuracy of air pollution exposure measurements: Statistical correction of a municipal low-cost airborne particulate matter sensor network," *Environ. Pollut.*, vol. 268, p. 115833, Jan. 2021, doi: 10.1016/J.ENVPOL.2020.115833.

[89] M. Si, Y. Xiong, S. Du, and K. Du, "Evaluation and calibration of a low-cost particle sensor in ambient conditions using machine-learning methods," *Atmos. Meas. Tech.*, vol. 13, no. 4, pp. 1693–1707, Apr. 2020, doi: 10.5194/AMT-13-1693-2020.

[90] I. Vajs, D. Drajic, N. Gligoric, I. Radovanovic, and I. Popovic, "Developing Relative Humidity and Temperature Corrections for Low-Cost Sensors Using Machine Learning," *Sensors 2021, Vol. 21, Page 3338*, vol. 21, no. 10, p. 3338, May 2021, doi: 10.3390/S21103338.

[91] J. Bi, A. Wildani, H. H. Chang, and Y. Liu, "Incorporating Low-Cost Sensor Measurements into High-Resolution PM2.5 Modeling at a Large Spatial Scale," *Environ. Sci. Technol.*, vol. 54, no. 4, pp. 2152–2162, Feb. 2020, doi: 10.1021/ACS.EST.9B06046/ASSET/IMAGES/LARGE/ES9B06046_0002.JPEG.

[92] F. E. Ahangar, F. R. Freedman, and A. Venkatram, "Using Low-Cost Air Quality Sensor Networks to Improve the Spatial and Temporal Resolution of Concentration Maps," *Int. J. Environ. Res. Public Heal. 2019, Vol. 16, Page 1252*, vol. 16, no. 7, p. 1252, Apr. 2019, doi: 10.3390/IJERPH16071252.

[93] P. Gupta *et al.*, "Impact of California Fires on Local and Regional Air Quality: The Role of a Low-Cost Sensor Network and Satellite Observations," *GeoHealth*, vol. 2, no. 6, pp. 172–181, Jun. 2018, doi: 10.1029/2018GH000136.

[94] C. C. Lim *et al.*, "Mapping urban air quality using mobile sampling with low-cost sensors and machine learning in Seoul, South Korea," *Environ. Int.*, vol. 131, p. 105022, Oct. 2019, doi: 10.1016/J.ENVINT.2019.105022.

[95] X. Liu *et al.*, "Low-cost sensors as an alternative for long-term air quality monitoring," *Environ. Res.*, vol. 185, p. 109438, Jun. 2020, doi: 10.1016/J.ENVRES.2020.109438.

[96] C. Malings *et al.*, "Fine particle mass monitoring with low-cost sensors: Corrections and long-term performance evaluation," *Aerosol Sci. Technol.*, vol. 54, no. 2, pp. 160–174, Feb. 2020, doi: 10.1080/02786826.2019.1623863/SUPPL_FILE/UAST_A_1623863_SM6450.XLSX.

[97] L. Shindler, "Development of a low-cost sensing platform for air quality monitoring: application in the city of Rome," *Environ. Technol.*, vol. 42, no. 4, pp. 618–631, 2021, doi: 10.1080/09593330.2019.1640290.

[98] J. Hofman *et al.*, "Spatiotemporal air quality inference of low-cost sensor data: Evidence from multiple sensor testbeds," *Environ. Model. Softw.*, vol. 149, p. 105306, Mar. 2022, doi: 10.1016/J.ENVSOFT.2022.105306.

[99] R. E. Connolly *et al.*, "Long-term evaluation of a low-cost air sensor network for monitoring indoor and outdoor air quality at the community scale," *Sci. Total Environ.*, vol. 807, p. 150797, Feb. 2022, doi: 10.1016/J.SCITOTENV.2021.150797.

[100] R. Dubey *et al.*, "Evaluation of low-cost particulate matter sensors OPC N2 and PM Nova for aerosol monitoring," *Atmos. Pollut. Res.*, vol. 13, no. 3, p. 101335, Mar. 2022, doi: 10.1016/J.APR.2022.101335.

[101] R. Williams *et al.*, “Air Sensor Guidebook,” 2022. [Online]. Available: www.epa.gov/ord.
[102] J. Li, S. K. Mattewal, S. Patel, and P. Biswas, “Evaluation of Nine Low-cost-sensor-based Particulate Matter Monitors,” *Aerosol Air Qual. Res.*, vol. 20, no. 2, pp. 254–270, Feb. 2020, doi: 10.4209/AAQR.2018.12.0485.
[103] K. Johnson, A. Holder, and A. Clements, “Development and Performance Validation of U.S. Wide Correction Equation for PurpleAir Sensor Data,” 2020.
[104] K. K. Barkjohn, B. Gantt, and A. L. Clements, “Development and application of a United States-wide correction for PM2.5 data collected with the PurpleAir sensor,” *Atmos. Meas. Tech.*, vol. 14, no. 6, pp. 4617–4637, Jun. 2021, doi: 10.5194/AMT-14-4617-2021.
[105] Y. Romero, R. M. Arias Velásquez, and J. Noel, “Development of a multiple regression model to calibrate a low-cost sensor considering reference measurements and meteorological parameters,” 2020, doi: 10.1007/s10661-020-08440-w.
[106] P. Strauß, M. Schmitz, R. Wöstmann, and J. Deuse, “Enabling of Predictive Maintenance in the Brownfield through Low-Cost Sensors, an IIoT-Architecture and Machine Learning,” *Proc. - 2018 IEEE Int. Conf. Big Data, Big Data 2018*, pp. 1474–1483, Jan. 2019, doi: 10.1109/BIGDATA.2018.8622076.
[107] K. Yamamoto, T. Togami, N. Yamaguchi, and S. Ninomiya, “Machine Learning-Based Calibration of Low-Cost Air Temperature Sensors Using Environmental Data,” *Sensors 2017, Vol. 17, Page 1290*, vol. 17, no. 6, p. 1290, Jun. 2017, doi: 10.3390/S17061290.
[108] S. Batterman, J. Burke, V. Isakov, T. Lewis, B. Mukherjee, and T. Robins, “A Comparison of Exposure Metrics for Traffic-Related Air Pollutants: Application to Epidemiology Studies in Detroit, Michigan,” *Int. J. Environ. Res. Public Health*, vol. 11, no. 9, p. 9553, Sep. 2014, doi: 10.3390/IJERPH110909553.
[109] IMIP, “Directorio Industrial de Ciudad Juárez.” http://www.imip.org.mx/directorio/ (accessed Oct. 20, 2022).
[110] I. Manisalidis, E. Stavropoulou, A. Stavropoulos, and E. Bezirtzoglou, “Environmental and Health Impacts of Air Pollution: A Review,” *Front. Public Heal.*, vol. 8, p. 14, Feb. 2020, doi: 10.3389/FPUBH.2020.00014.
[111] Z. Yong and Z. Haoxing, “Digital universal particle concentration sensor PMS5003 series data manual,” 2016.
[112] J. L.Tipper, L. Richards, E. Ingham, and J. Fisher, “Characterization of UHMWPE Wear Particles,” *UHMWPE Biomater. Handb.*, pp. 409–422, 2009, doi: 10.1016/B978-0-12-374721-1.00027-4.
[113] Y. A. Eremin, “Scattering: Scattering Theory,” *Encycl. Mod. Opt. Five-Volume Set*, pp. 326–330, Jan. 2004, doi: 10.1016/B0-12-369395-0/00682-5.
[114] AQ-SPEC, “AQ-SPEC,” 2022. http://www.aqmd.gov/aq-spec/evaluations/summary-pm (accessed Aug. 29, 2022).
[115] PurpleAir, “PurpleAir, Inc.,” 2022. https://www2.purpleair.com/community/faq#hc-how-do-purpleair-sensors-work (accessed Sep. 07, 2022).
[116] M. Eeftens *et al.*, “Development of land use regression models for nitrogen dioxide, ultrafine particles, lung deposited surface area, and four other markers of particulate matter pollution in the Swiss SAPALDIA regions,” *Environ. Heal. A Glob. Access Sci. Source*, vol. 15, no. 1, pp. 1–14, Apr. 2016, doi: 10.1186/S12940-016-0137-9/TABLES/6.
[117] R. N. Forthofer, E. S. Lee, and M. Hernandez, “Linear Regression,” *Biostatistics*, pp. 349–386, 2007, doi: 10.1016/B978-0-12-369492-8.50018-2.
[118] N. Pandis, “Correlation and linear regression,” *Am. J. Orthod. Dentofac. Orthop.*, vol.

149, no. 2, pp. 298–299, Feb. 2016, doi: 10.1016/j.ajodo.2015.11.010.
[119] M. Attenborough, “Functions and their graphs,” *Math. Electr. Eng. Comput.*, pp. 26–56, 2003, doi: 10.1016/B978-075065855-3/50028-0.
[120] A. W. Moore, B. Anderson, K. Das, and W. K. Wong, “Combining Multiple Signals for Biosurveillance,” *Handb. Biosurveillance*, pp. 235–242, 2006, doi: 10.1016/B978-012369378-5/50017-X.
[121] P. R. Story, D. W. Galipeau, and R. D. Mileham, “A study of low-cost sensors for measuring low relative humidity,” *Sensors Actuators B Chem.*, vol. 25, no. 1–3, pp. 681–685, Apr. 1995, doi: 10.1016/0925-4005(95)85150-X.
[122] S. Feinberg *et al.*, “Long-term evaluation of air sensor technology under ambient conditions in Denver, Colorado,” *Atmos. Meas. Tech.*, vol. 11, no. 8, pp. 4605–4615, Aug. 2018, doi: 10.5194/AMT-11-4605-2018.
[123] R. Jayaratne, X. Liu, P. Thai, M. Dunbabin, and L. Morawska, “The influence of humidity on the performance of a low-cost air particle mass sensor and the effect of atmospheric fog,” *Atmos. Meas. Tech*, vol. 11, pp. 4883–4890, 2018, doi: 10.5194/amt-11-4883-2018.
[124] N. Karaoghlanian, B. Noureddine, N. Saliba, A. Shihadeh, and I. Lakkis, “Low cost air quality sensors ‘PurpleAir’ calibration and inter-calibration dataset in the context of Beirut, Lebanon,” *Data Br.*, vol. 41, p. 108008, Apr. 2022, doi: 10.1016/J.DIB.2022.108008.
[125] G. Tancev, “Relevance of drift components and unit-to-unit variability in the predictive maintenance of low-cost electrochemical sensor systems in air quality monitoring,” *Sensors*, vol. 21, no. 9, p. 3298, May 2021, doi: 10.3390/S21093298/S1.
[126] H. Y. Liu, P. Schneider, R. Haugen, and M. Vogt, “Performance assessment of a low-cost PM 2.5 sensor for a near four-month period in Oslo, Norway,” *Atmosphere (Basel).*, vol. 10, no. 2, Jan. 2019, doi: 10.3390/ATMOS10020041.
[127] C. Malings *et al.*, “Development of a general calibration model and long-term performance evaluation of low-cost sensors for air pollutant gas monitoring,” *Atmos. Meas. Tech.*, vol. 12, no. 2, pp. 903–920, Feb. 2019, doi: 10.5194/AMT-12-903-2019.
[128] Y. Su, “Linear regression results of the FEM SHARP 5030 vs the FRM at the... | Download Table,” 2018, Accessed: Nov. 01, 2022. [Online]. Available: https://www.researchgate.net/figure/Linear-regression-results-of-the-FEM-SHARP-5030-vs-the-FRM-at-the-Toronto-West-station_tbl2_325204839.
[129] S. M. Bortnick, “Journal of the Air & Waste Management Association Using Continuous PM 2.5 Monitoring Data to Report an Air Quality Index) Using Continuous PM 2.5 Monitoring Data to Report an Air Quality Index,” *J. Air Waste Manage. Assoc.*, vol. 52, no. 1, pp. 104–112, 2002, doi: 10.1080/10473289.2002.10470763.
[130] N. Cheng *et al.*, “Spatio-temporal variations of PM2.5 concentrations and the evaluation of emission reduction measures during two red air pollution alerts in Beijing,” *Sci. Rep.*, vol. 7, no. 1, Dec. 2017, doi: 10.1038/S41598-017-08895-X.
[131] V. Singh, S. Singh, A. Biswal, A. P. Kesarkar, S. Mor, and K. Ravindra, “Diurnal and temporal changes in air pollution during COVID-19 strict lockdown over different regions of India,” *Environ. Pollut.*, vol. 266, p. 115368, Nov. 2020, doi: 10.1016/J.ENVPOL.2020.115368.
[132] M. I. Manning, R. V. Martin, C. Hasenkopf, J. Flasher, and C. Li, “Diurnal Patterns in Global Fine Particulate Matter Concentration,” *Environ. Sci. Technol. Lett.*, vol. 5, no. 11, pp. 687–691, Nov. 2018, doi:

10.1021/ACS.ESTLETT.8B00573/SUPPL_FILE/EZ8B00573_SI_001.PDF.

APPENDIX

Table 22: PM_{10} Summary Statistics

Sensor	Average	Standard Deviation	Minimum	Maximum
Zavala	3.74	4.67	0.01	53.69
ZavalaEs	13.15	15.6	0.14	164.2
Hawkins	4.82	6.18	0.23	139.6
Bonham	5.27	7.19	0.58	158.43
Douglass	5.1	5.72	0.17	79.07
Coldwell	4.06	5.35	0.02	97.08
Aoy	14.5	18.1	0.26	185.4
AoyES	6.48	8.98	0.22	157.07
Mesita	4.07	5.36	0.04	92.7
Cielo Vista	6.77	8.36	0.35	180.83
Park2	4.52	4.84	0.05	57.73
ParkES	3.68	5.32	0	97.67
Whitaker	4.31	5.55	0.03	111.82
Western Hills	3.51	4.4	0	59.15
Zach White	4.77	5.84	0.05	79.38
UTEP 3	4.14	4.46	0.07	48.3
UTEP 2	5.15	6.63	0.05	100.55
UTEP 1	5.55	5.33	0.29	57.23
UACJ-PAC07	-	-	-	-
UACJ-PAC13	9.47	13.19	0.3	212.93
UACJ-PAC16	8.04	12.72	0.11	220.54
UACJ-PAC11	5.08	5.38	0.27	52.3
UACJ-PAC08	5.84	7.84	0.08	116.62
UACJ-PAC22	4.51	7.71	0.06	125.88
UACJ-PAC21	4.64	7.76	0.02	113.7
UACJ-PAC20	4.48	6.14	0.03	108.07
UACJ-PAC19	7.57	8.69	0.26	166.93
UACJ-PAC04	6.89	10.54	0.14	143.7
UACJ-PAC23	7.52	10.36	0.14	123.19
UACJ-PAC24	9.65	7.95	0.61	69.66
UACJ-PAC26	7.62	6.38	1.12	61.17
UACJ-PAC25	7	6.46	0.12	54.65
UACJ01	5.97	6.6	0.23	100.77
UACJ-PAC12	-	-	-	-
UACJ-PAC09	6.22	9.08	0.11	143.58
UACJ-PAC10	6.13	8.37	0.05	116
UACJ-PAC01	11.62	14.88	0.5	281.95
UACJ-PAC15**	6.43	6.1	0.13	55.15
UACJ-PAC28	7.48	9.85	0.07	112.7
UACJ-PAC14**	8.5	6.95	1.19	66.36
UACJ-PAC27	8.22	12.58	0.09	202.02
UACJ-PAC02	120.3	748.7	0.42	5554.3
UACJ-PAC03	7.38	6.79	0.73	64.68
UACJ-PAC17	4.7	7.8	0.02	114
UACJ-PAC18	-	-	-	-
UACJ-PAC05	7.71	10.03	0.37	158.51
UACJ-PAC06	5.31	9.75	0.04	163.63

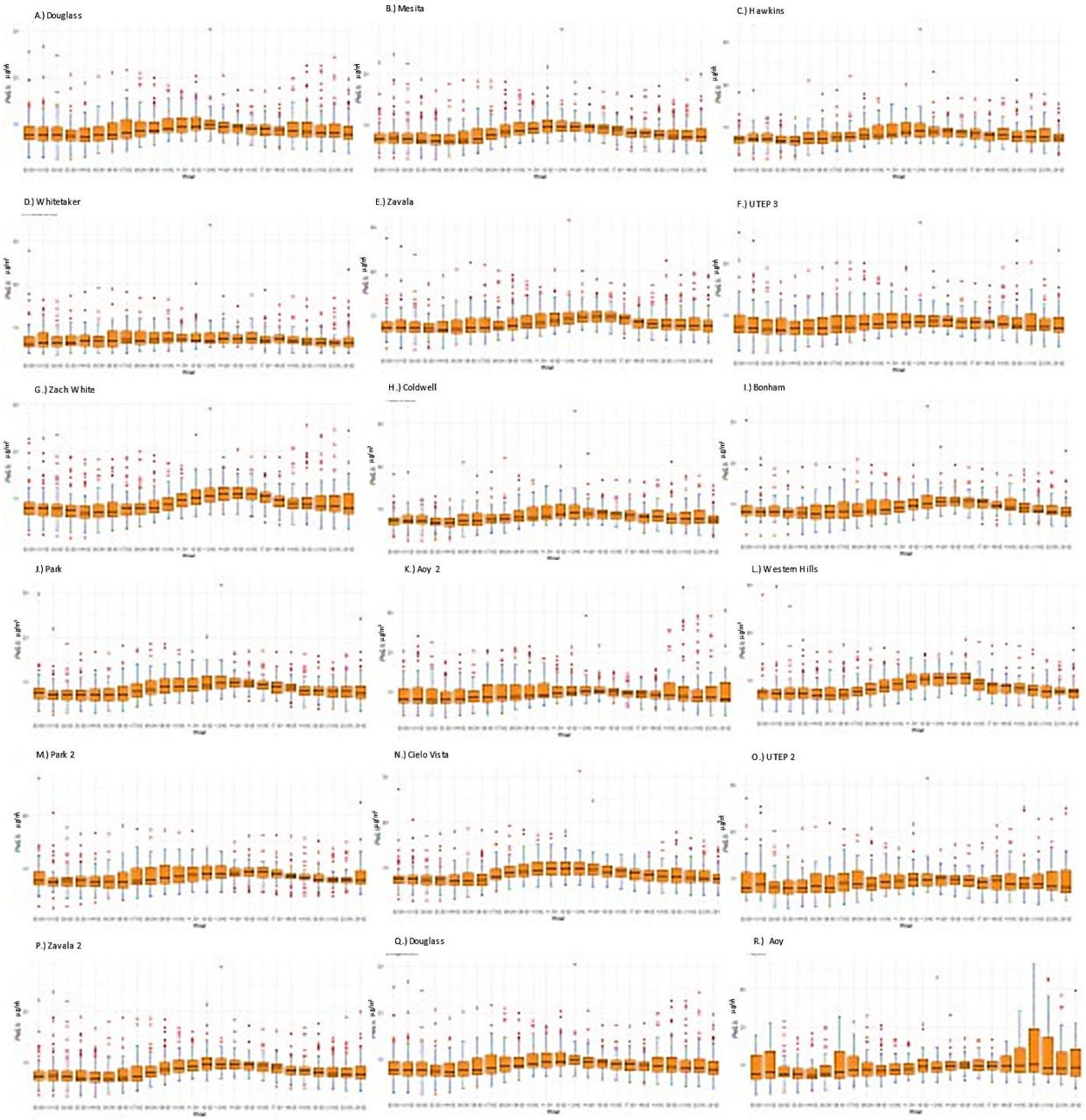

Figure 10: Diurnal Variation Box Plots For El Paso Texas

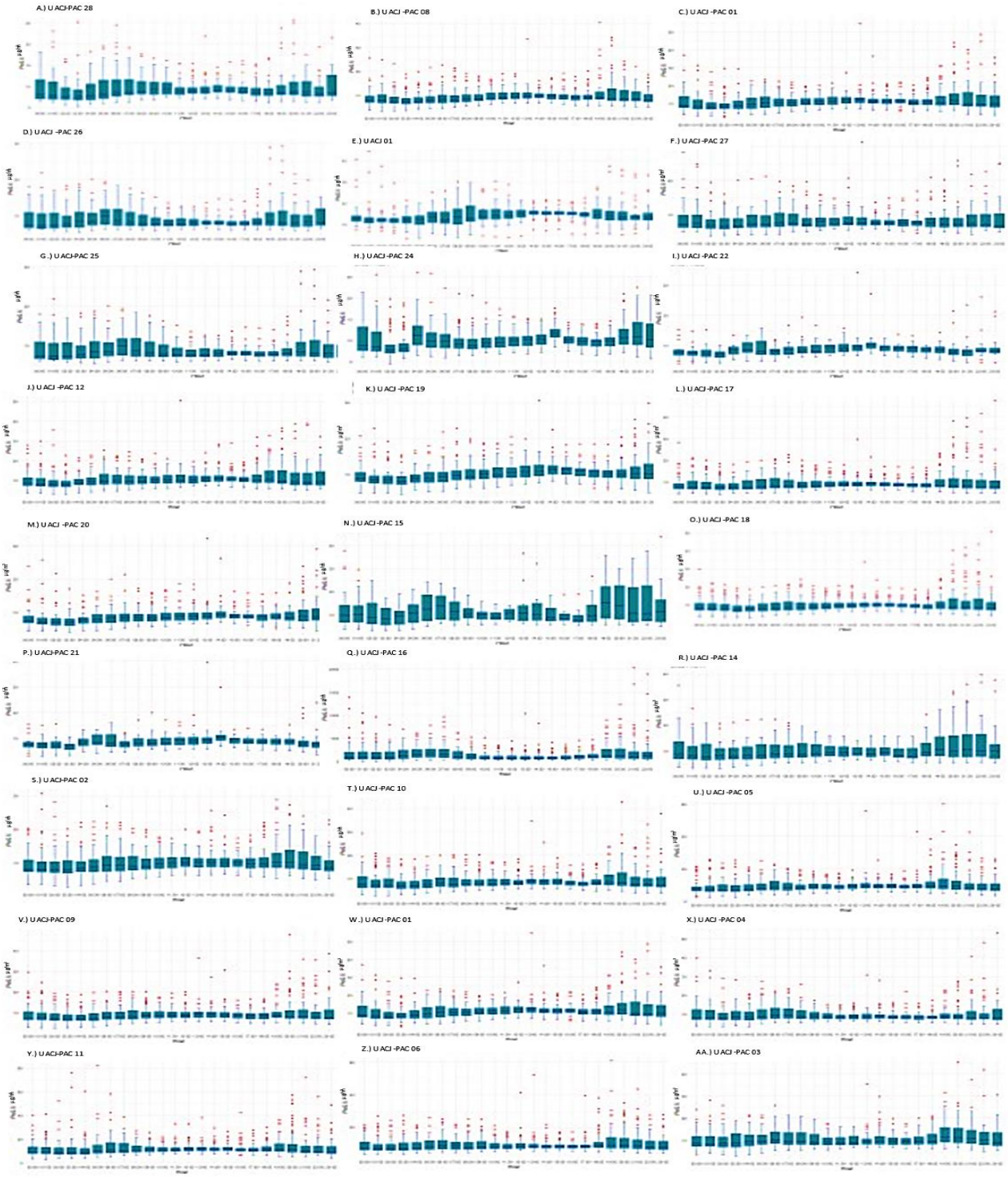

Figure 11: Diurnal Variation Box Plots for Cd. Juarez Mexico

VITA

Leonardo D. Vazquez-Raygoza was born in El Paso, Texas. While attending Valle Verde Early College High School, he obtained his Associates of Arts from El Paso Community College in 2017. After graduating from Valle Verde Early College High School, he attended the University of Texas at El Paso from 2017-2022. He received his Bachelor of Science degree in Civil Engineering and pursued a graduate degree in Master of Science in Civil Engineering.

During 2018-2019 he worked as an undergraduate research assistant for Dr. Shane Walker in the Center for Inland Desalination Systems. During his time in the CIDS laboratory, he worked on colorimetric water analysis and work regarding wastewater treatment using electrodialysis. . He received an internship with CDM Smith in the Fall of 2020; during this internship, he assisted with the development of a model of a full-scale brackish desalination system for the water reuse plant in Fabens, Texas.

Following the internship, he worked as a research and teaching assistant for Dr. Wen-Whai Li from 2020-2022. As a research assistant, he has worked on several projects involving monitoring criteria pollutants in the El Paso del Norte Region and assisting in a bi-national collaboration with the Universidad Autonoma de Ciudad Juarez in project grants provided by the EPA and TCEQ. In addition, in 2021, he was awarded the Dwight David Eisenhower Transportation Fellowship.